Hindawi
Journal of Advanced Transportation
Volume 2023, Article ID 6658030, 23 pages
https://doi.org/10.1155/2023/6658030

Research Article

Minimum Cost Flow-Based Integrated Model for Electric Vehicle and Crew Scheduling

Yindong Shen [1,2] **and Yuanyuan Li** [1,2]

[1]*School of Artificial Intelligence and Automation, Huazhong University of Science and Technology, Wuhan 430074, China*
[2]*Key Laboratory of Image Processing and Intelligent Control, Huazhong University of Science and Technology, Ministry of Education, Wuhan, China*

Correspondence should be addressed to Yindong Shen; yindong@hust.edu.cn

Received 21 June 2023; Revised 8 October 2023; Accepted 17 October 2023; Published 1 November 2023

Academic Editor: Tao Liu

Vehicle and crew scheduling is vital in public transit planning. Conventionally, the issues are handled sequentially as the vehicle scheduling problem (VSP) and crew scheduling problem (CSP). However, integrating these planning steps offers additional flexibility, resulting in improved efficiency compared with sequential planning. Given the ever-growing market share of electric buses, this paper introduces a new model for integrated electric VSP and CSP, called EVCSPM. This model employs the minimum cost flow formulations for electric VSP, set partitioning for CSP, and linking constraints. Due to the nonlinear integer property of EVCSPM, we propose a method that hybrids a matching-based heuristic and integer linear programming solver, GUROBI. The numerical results demonstrate the efficiency of our methodology, and the integrated model outperforms the sequential model in real-life scenarios.

1. Introduction

Developing public transit is the fundamental way to achieve sustainable urban development [1], which has been a widely discussed topic since the 1960s. Specifically, vehicle and crew scheduling are two major planning problems in public transport scheduling [2]. These problems aim at minimizing the operational costs associated with the fleet size and crew size required to ensure timely trips and compliance with labor crew regulations for efficient vehicle blocks and crew shifts [3]. Typically, these problems are approached separately, with the vehicle scheduling problem being addressed first, followed by the crew scheduling problem [4].

Ball et al. [5] contend that scheduling vehicles independently of the crew is not ideal for urban transportation, as crew cost typically outweighs vehicle operating cost. It is well established that integrating planning steps reveals more options and increases the solution space, leading to greater efficiency gains [6].

Furthermore, public transport operators face challenges transitioning from conventional diesel to electric vehicles (EVs) powered by batteries [7]. In recent years, the market share of EVs has experienced a significant increase [8–10]. On the 27th of January 2022, the Ministry of Transport issued the "14th Five-year Development Plan for Green Transportation," which includes a goal of reaching 72% of EVs in urban public transport and making fully EVs the mainstream option in the bus market by 2025 [11]. Hence, we address the electric VSP (EVSP) and CSP simultaneously. The combination of these two problems is called the electric vehicle and crew scheduling problem (EVCSP).

Resource-constrained VSPs, including EVSP, are known to be NP-hard [12]. In addition, the single-based CSP is also NP-hard due to complex constraints arising from wage agreements and internal regulations [13]. The EVCSP falls into the category of NP-hard problems. It is considerably more challenging than the isolated problem [14], and it takes more time to solve optimally, particularly for real-world and large-size applications [15].

Only a few papers tackle the integrated vehicle and crew scheduling problem (VCSP) [4], and several discussions concern the electric version (EVCSP). Existing literature on VCSP (including EVCSP) models and algorithms is summarized in Table 1. To our knowledge, all models proposed in the literature fall into one of two classes [55]: (i) partial integrations and (ii) complete integrations that require decisions to be taken simultaneously.

Some early papers deal with partial integration [33]: (1) schedule vehicles using a heuristic approach in CSP, (2) include crew considerations in VSP, and (3) change vehicle schedules in CSP. Most of the procedures fall under the first category and are based on a heuristic procedure proposed by Ball and Bodin [5]. The solution procedure is decomposed into three components, emphasizing the CSP: a piece construction component, a piece improvement component, and a shift generation component. Similar heuristic approaches in the first category are proposed by Tosini and Vercellis [23]; Falkner and Ryan [21]; and Patrikalakis and Xerocostas [22]. All these approaches use a similar set covering formulations as in Ball et al. [5]. Afterward, the approach that solves CSP incorporates side constraints for the vehicles that appear [4]. Scott [18] first proposed approaches for the second category by heuristically determining vehicle schedules that account for crew costs using the linear programming dual of the HASTUS CSP model. The third category has far fewer fruits than the first two, with Gintner et al. [26] proposing a time-space network formulation for CSP that allows vehicles to have more autonomy during the crew scheduling phase, ultimately leading to selecting the most consistent vehicle schedule that aligns with the objectives of CSP. We refer to Freling et al. [28] for an overview of these papers.

The state-of-the-art complete integration models for VCSP fall into three main categories [50]: (1) network-flow-based formulation, (2) constraint-based model, and (3) maximum covering model. The earliest and most successful category is the network-flow-based formulation. These models mainly comprise time-space/multicommodity/quasi-assignment [2, 4, 38] network flow formulations for VSP, a set partitioning/covering for CSP, and additional linking constraints to ensure the compatibility of vehicle and crew schedules [14]. Freling [29] introduces the first integrated VCSP model using quasi-assignment-based formulations, while Huisman [27] provides the initial general formulations for VCSP by extending the single-depot model of Freling [29] to the multidepot case. The second category of models can refer to Laurent and Hao [53] who present an integrated model based on constraint satisfaction that is intuitive and natural [3]. Prata et al. [56–58] propose the maximal covering model under the third category, which generates potential blocks, shifts directly over the timetabled trips, and then covers all trips with available resources (vehicles and crews). For an overview of complete integration, we can refer to Steinzen et al. [42].

To the best of our knowledge, only two papers address the issue of EVCSP: Perumal et al. [7] and Sistig and Sauer [34]. Perumal et al. [7] modify the mathematical model proposed by Friberg and Haase [20] to explain VCSP as a set partitioning problem by adding additional constraints that link vehicle and crew schedules. They incorporate the crucial constraints of EVs, including limited driving range and lengthy recharging times [60, 61], into the VCSP, thereby increasing operational complexity. Their research suggests resolving EVCSP using a branch-and-price heuristics method coupled with an adaptive large neighborhood search (ALNS). However, the model referred to by Perumal et al. [7] is partially integrated and only considers a constant driving range for EVs. Yet, the actual driving range can be influenced by various factors such as air density, driving speed, air conditioning usage, and complex road surfaces [11]. Then, Sistig and Sauer [34] avoid this flaw, and the integrated model they refer to is initially proposed by Freling [29]. This paper aims at an innovative, low-complexity model for the integrated issue and advocates for energy consumption and recharging strategies that are more practical to include in the scheduling process.

The minimum cost flow (MCF) is a common type of network flow that can be extended in various ways [62]. This paper presents a complete integration model for EVCSP, which is based on the MCF. Specifically, the model involves MCF formulations for EVSP, set partitioning for CSP, and linking constraints that guarantee compatibility of EV and crew schedules. The outcomes of MCF can be useful for addressing various network-related issues, including maximum flow, assignment, shortest path, transshipment, and transportation problems [63]. Successful integration requires a practical design of the key MCF components.

Furthermore, it is imperative to customize EVs' energy consumption and charging strategy for accurate modeling. In practice, EVs spend significant time at multiple intermediate stops, waiting at red lights, and navigating through traffic jams. Thus, we divide the EV operation into prevailing driving and standstill. Fontana [64] demonstrates that the energy consumption of an EV is modeled using engineering principles and supported by analytics. We utilize the mentioned model to calculate the EV energy consumption of prevailing driving and standstill states. Typically, EV charging strategies include battery swaps, slow recharge, and fast recharge [60, 61]. The current mainstream strategy in bus operation enterprises is to perform slow recharge at night and fast recharge during daily operations [11].

The contributions of this research are fivefold: (a) A novel EVCSP model based on MCF is proposed with an integrated design for nodes, directed arcs, cost, and constraints; (b) the exact minimum fleet size for VCSP is derived, and furthermore, the lower bound of both fleet and crew sizes for EVCSP is discussed since minimizing fleet and crew sizes are the primary task; (c) time compatibility and energy compatibility of any two spells or trips are defined for arc generation; (d) an approach hybrids a matching-based heuristic method, and integer linear programming (ILP) solver is derived for our integrated model; and (e) a series of numerical examples are provided to illustrate the performance of the model and the approach developed.

The remainder of the paper is structured as follows. Section 2 elaborates on the concepts related to EVCSP. Section 3 suggests an integrated design for the problem

Table 1: A summary of the studies related to the integrated VCSP models and algorithms.

Type	Publication	Model	Approach
Include crew considerations in VSP	[16–18]	LP dual	Heuristic
	[19, 20]	SP & CSP constraints	Branch and price
	[7] (EVCSP)	SP & CSP constraints	Adaptive large neighborhood search
Schedule vehicles heuristically in CSP	[5]	SP	Matching heuristic
	[21–23]	SC	Heuristic
	[24]	SP	Branch and cut and price
	[14, 25]	SP & side constraints	Branch and price
	[4]	SP & side constraints	Lagrangian heuristic
Change vehicle schedule in CSP	[26]	TSF	Column generation
Complete integration	[26] (No changeovers), [27]	SC	Heuristic
	[4, 28–33], [34] (EVCSP), [35]	QAF & SP	Lagrangian heuristic
	[36]	MCF & SP	Lagrangian heuristic
	[37–40]	MCF & SP/SC	Column generation & branch and bound/price
	[41] (considering delays)	MCF & SP	Column generation
	[42]	MCF & SP	Hybrid evolutionary
	[43]	MCF & SP	Bundle method
	[44]	MCF & SP	Splitting method
	[45] (no changeovers)	MCF & SP	Valid inequality & CPLEX
	[46]	MCF & SC	—
	[47, 48]	MCF & SC	Decomposition approach
	[6]	MCF & SP	Heuristic
	[2]	TSF & SP	Column generation & Lagrangian relaxation
	[49] (Considering delays), [50]	TSF & path-based formulations	Lagrangian heuristic
	[51]	TSF & SP	Branch and price
	[52]	TSF	Matheuristic
	[53]	CM	Simulated annealing
	[54]	CM	Greedy randomized adaptive search
	[55]	CM	Variable neighborhood search
	[3] (considering the crew's reliability)	CM	Variable neighborhood search
	[56] (no changeovers)	MCM	Heuristic
	[57, 58]	MCM	Hybrid evolutionary
	[59]	RSP	Column generation-based approach

[a]SC/SP: set covering/set partitioning. [b]TSF: time-space network flow. [c]MCF: multicommodity network flow. [d]QAF: quasi-assignment network flow. [e]MCM: maximum covering model. [f]CM: constraint-based model. [g]LP: linear programming. [h]RSP: resource-constrained shortest path.

based on MCF. Section 4 presents the EVCSP model and provides some statements. Section 5 presents the hybrid heuristic method for the model. Section 6 displays the numerical experimental results and sensitivity analyses based on a realistic dataset. Finally, Section 7 provides concluding remarks and suggests future work.

2. Electric Vehicle and Crew Scheduling Problem

The EV and crew Scheduling can be clarified more clearly by breaking it into subproblems and giving an integrated description. We initially establish the concepts by introducing the following terminologies [1, 65]:

Trip: A trip refers to the task unit, which includes a start time at the departure point, an end time at the arrival point, and a duration known as trip time.

Block: A block is a vehicle's task to start from a depot, followed by a sequence of trips, and ends at the depot.

Relief opportunity (RO): RO is a time/location pair where crews can be relieved. The time is a relief time, and the location is a relief point. EVs use only some ROs to relieve crews. Crews are required to take relief at specific relief points, usually determined by public transport companies. Depending on the circumstances, the crew's movement between these relief points can be organized by the transportation enterprise or the crew itself.

Piece: A piece is a work done between two consecutive ROs during which crews do not have an RO.

Spell: A spell consists of multiple consecutive pieces within a vehicle block, all handled by a single crew without relief from other crews.

Shift: A shift refers to the assignment of multiple spells to a single crew. A crew's task starts from a depot, followed by several spells, and ends at the depot. Shifts encompass split, straight, and tripper shifts. The split shift has a long length and a long break, while the tripper shift has a short length but no break. The straight shift has a short break.

Idle time: Idle time refers to the waiting time between two consecutive trips.

Deadhead: Deadhead is the empty movement between any two consecutive *trips* of a vehicle.

2.1. Electric Vehicle Scheduling Problem. Compared to the traditional VSP for fueled vehicles, the EVSP is more intricate because an EV's battery capacity is restricted, requiring specific recharging points that involve a prolonged time.

The EVSP involves generating several *blocks* and assigning each to an EV. The *blocks* are constructed by organizing the EV's daily work, starting from a pull-out from a depot, followed by a sequence of *trips*, and ending at a pull-in to the same depot. The objective is to minimize fleet size and variable operating costs, which include *trip times*, *idle times*, and *deadheads* [66]. The optimization is subject to three constraints:

(a) Each *trip* can only be assigned to one EV

(b) Each EV must begin and end its daily work with a pull-out from and pull-in to the same depot, respectively

(c) Two consecutive trips for each EV must be time- and energy-compatible

Figure 1 depicts the EVSP in a time-space network. The *trips* comprise three departure (or arrival) points, namely P_1, P_2, and P_3. D represents the set of depots, and R represents the set of recharge points. There are four types of arcs in the network: a pull-out arc connects a depot to a *trip*, a pull-in arc connects a *trip* to a depot, a trip-link arc connects two *trips*, and a recharge-link arc connects a *trip* to another *trip* through a visit to a hidden recharge point. An EV has to temporarily return to a depot, also known as a depot return when the gap between two consecutive *trips* is significant. Maintaining the EV's energy during scheduling via recharging is imperative.

2.2. Crew Scheduling Problem. Crew scheduling aims to create a feasible schedule (several *shifts*) to cover all tasks within a single day of vehicles (all *blocks*). The objectives of CSP are twofold: minimize both the crew size and the total wage costs while adhering to the following constraints:

(a) Each *trip* is assigned to a single *shift*

(b) Each crew's relief occurs at the specified *RO*

(c) Each *shift* must confirm all operational requirements and labor laws, known as a *legal shift*

The labor laws pertaining to the CSP are intricate and multifaceted. Below, we provide a summary of typical constraints that restrict the efficacy of shifts:

(1) The length of a *spell* must not exceed the stipulated upper limit

(2) The length of a *shift* should not surpass the maximum length designated for the respective *shift* type

(3) The working hours for a *shift* must fall within the minimum and maximum limits specified for the corresponding *shift* type

(4) The driving time during a *shift* should not exceed the minimum and maximum driving time allowances set for the respective *shift* type

(5) During a straight *shift*, meal breaks must be taken at the designated time and location

(6) For split *shifts*, check-in and check-out times must not occur earlier than the earliest check-in time nor later than the latest check-out time prescribed

Figure 2 details the composition of three 2-*spell shifts* pertaining to some EV work.

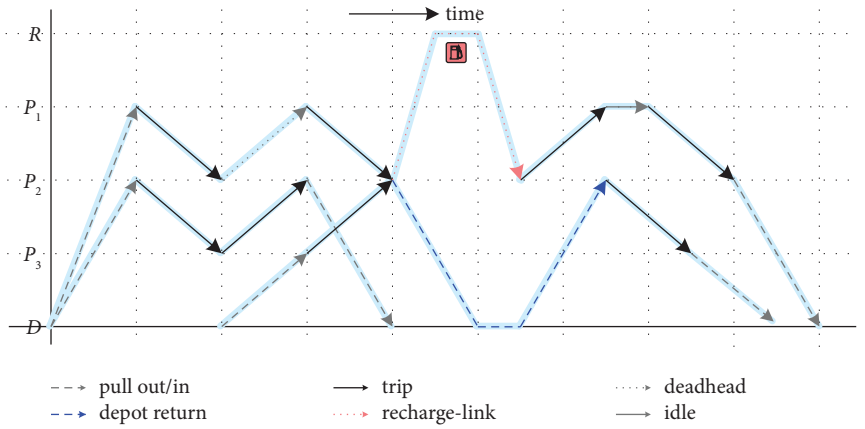

Figure 1: A time-space network flow for the EVSP.

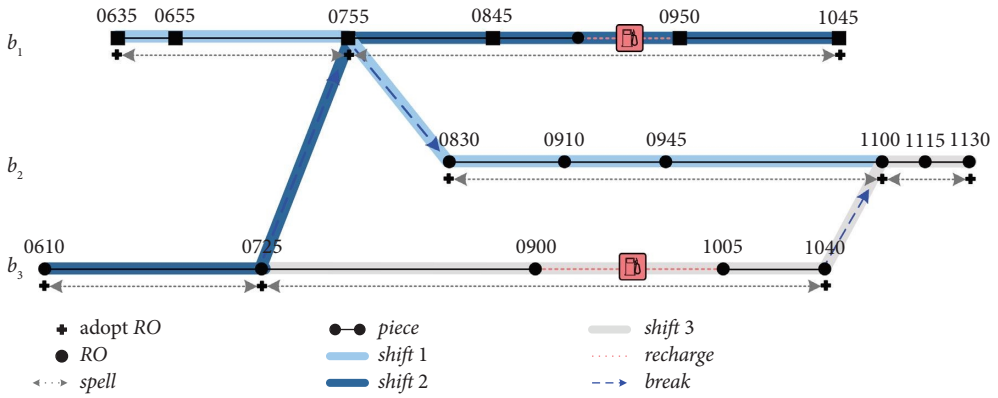

Figure 2: Illustration of the composition of 2-*spell shifts* with the EV *blocks* b_1, b_2, and b_3.

2.3. Integrated Electric Vehicle and Crew Scheduling Problem. EVCSP aims to generate a feasible schedule for EVs and crews to cover all tasks, i.e., all *trips*. The objectives of EVCSP are to minimize fleet size and crew size, *deadheading time*, *idle time*, and wage costs. The crews are permitted to carry out crossovers at relief points. The schedule is subject to complex constraints [67]. In particular, the following universal constraints must be satisfied:

(a) Each *trip* must be covered by only one EV

(b) Each EV must be handled by only one crew simultaneously, but another crew can replace the crew

(c) Each EV must start its first *trip* from a depot and end its daily work there

(d) The connection of any two consecutive EV trips must be compatible regarding time and energy

(e) Each crew's relief must be carried out at the specified *RO*

(f) Each shift must comply with all operational constraints and labor laws

This paper is dedicated to addressing the single depot EVCSP, where EVs are responsible for both pull-out and pull-in operations at a single depot. Figure 3 illustrates the EV *blocks* and crew *shifts* simultaneously from integrated EV and crew scheduling for executing the timetabled *trips* as shown in Figure 4.

2.4. Related Assertions of Fleet Size and Crew Size. Let $T = \{1, 2, \ldots, n\}$ denote the set of timetabled *trips*. This section introduces the notions related to time compatibility.

Definition 1 (Θ). Let t_i^s and t_i^e denote the start and end time of trip i, and DH_{ij} refers to the deadheading time from trip i to trip j. Bertossi et al. [68] define the compatibility $i\Theta j$ of any two trips, i and j, as

$$T_i^e + \mathrm{DH}_{ij} \le T_j^s. \tag{1}$$

Otherwise, trip i is time incompatible with trip j ($i\overline{\Theta}j$).

Definition 2 (Incompatible set). If $\exists U \subset T$, $\ni i\overline{\Theta}j$, $\forall i, j \in U$, then U is an incompatible set.

Definition 3 (Incompatible degree, ID). Suppose U is an incompatible set of T, then the number of trips in U is the incompatible degree, i.e., $\mathrm{ID}(U) = |U|$.

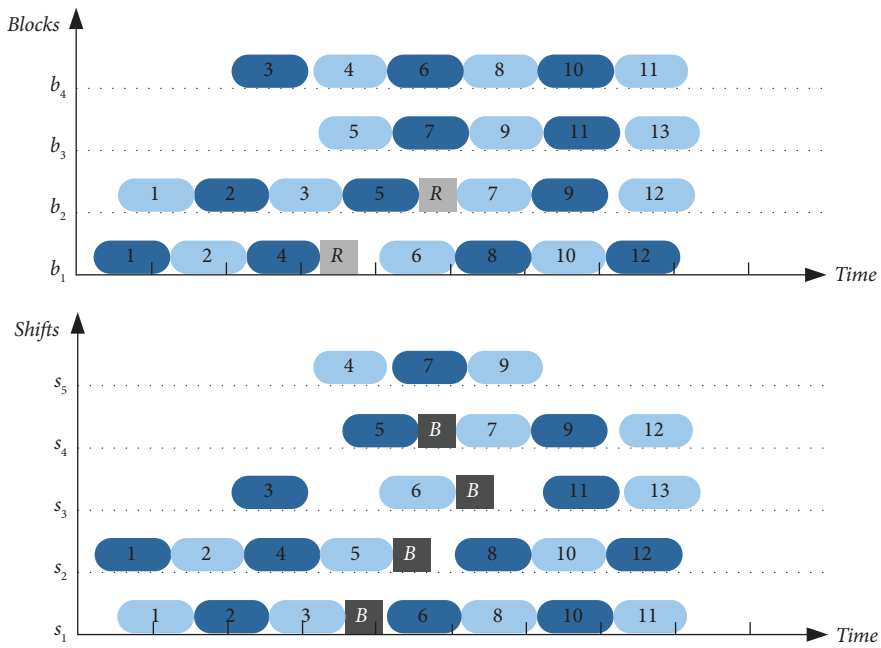

FIGURE 3: EV schedules b_1, b_2, b_3, b_4. Crew schedules s_1, s_2, s_3, s_4, s_5. R is the 30 min recharge of the EV. B is the legal 30 min break that the crew has to avoid working blocks of more than 4 h. The crew's working time cannot be up to 8 h.

Trips (*A*-*B*)	1	2	3	4	5	6	7	8	9	10	11	12
ST	6:15	7:35	8:05	8:15	9:35	10:10	10:15	11:05	12:05	12:10	12:15	13:05

Trips (*B*-*A*)	1	2	3	4	5	6	7	8	9	10	11	12	13
ST	6:35	7:15	8:35	9:10	9:15	10:05	11:05	11:10	11:15	12:05	13:10	13:15	13:20

FIGURE 4: The list of timetabled trips involves two departure (or arrival) points, A and B. A-B and B-A are two directions of the *trips*. The second line is the timetable for each *trip*. The *trip* time of each trip is 1 h. The deadheading time from A to B (or B to A) is 1 h.

Definition 4 (Maximum incompatible degree, MID). MID represents the largest ID among all incompatible sets of T, i.e., $\mathrm{MID}(T) = \max\{ID(U) \mid \forall \text{in compatible set } U \text{ of } T\}$.

By referring to the decomposition theorem [69], we derive the theoretical minimum fleet size (TMF) for the VCSP.

Theorem 6. *Let T be the set of timetabled trips. Then, the TMF for the VCSP is equal to MID(T).*

Proof. It is reasonable to assume that the set T, equipped with the time compatibility relation, forms a partially ordered set (poset). For a poset P, elements a and b are comparable only if either $a \leq b$ or $b \leq a$; otherwise, they are noncomparable. A subset S of P is called a chain if every two elements in S are comparable. A subset S of P is independent if every two elements in S are noncomparable. For the VCSP, we define a trip as an element in the poset and use the time compatibility of *trips* to establish the comparability relation. Then, a *block* corresponds to a chain. Dilworth's decomposition theorem states that the minimum number of chains partitioning a poset P equals the maximal number of independent elements. Consequently, the TMF for the VCSP is equivalent to $MID(T)$. Theorem 6 is true. □

Corollary 7. *For the EVCSP, MID(T) provides a lower bound for the fleet size.*

Proof. Since EVs have limited battery capacity, we need to consider both the nodes' time and energy compatibility (see Section 3.3). As a result, its fleet size is not less than that of VCSP. □

Proposition 8. *The EVCSP requires a crew size that is no less than $L = W/(S\text{-}A\text{-}B\text{-}C)$, where W is the total working time needed for timetabled trips, S is the maximum length of the spread over for a normal shift stipulated in the labor laws, and A and B denote the time allowances for crews to sign on and sign off at depot respectively, while C denotes the specified minimum meal break.*

Proof. The daily working time of a crew cannot exceed S-A-B-C. Hence, Proposition 8 is straightforwardly correct. □

3. Integrated Design for Electric Vehicle and Crew Scheduling Based on Minimum Cost Flow

In graph theory, MCF is a network with direct arcs and nodes. It requires a least-cost path starting from a given node, followed by several nodes connected by directed arcs, and ending at a specified node.

Let $G(N, A)$ be a directed network consisting of the arc cost c_{ij} and capacity (upper bound, u_{ij}, and lower bound, l_{ij}) associated with every arc (i, j) belonging to A. Each node $i \in N$ possesses several resources b_i. The MCF model (MCFM) can be formulated as follows:

$$(\textbf{MCFM}) \quad \min \quad f(x) = \sum_{(i,j)\in A} c_{ij} \cdot x_{ij}, \tag{2}$$

$$\text{s.t}\, l_{ij} \le x_{ij} \le u_{ij}, \quad \forall (i, j) \in A, \tag{3}$$

$$\sum_{j:(i,j)\in A} x_{ij} = \sum_{j:(j,i)\in A} x_{ji} = b(i), \quad \forall i \in N, \tag{4}$$

$$x_{ij} \ge 0 \text{ and integer}, \quad \forall (i, j) \in A. \tag{5}$$

The objective is to minimize the total cost, with the capacity constraint and conservation of flows represented by (3) and (4), respectively. If arc (i, j) is selected, $x_{ij} > 0$; otherwise, $x_{ij} = 0$. We now develop an integrated design for EVSP and CSP based on the MCF.

3.1. Integrated Design for EVCSP. We design four critical elements to transform EVCSP into an MCF problem: nodes, directed arcs, cost, and constraints.

Incorporating both the EV and crew constraints, along with their associated limitations, into the EVCSP model presents significant complexity, and thus, building the model directly becomes difficult. As a result, we employ a design based on a set of predetermined *potential shifts*, which act as the precondition for the integrated EVCSP model (EVCSPM).

Statement 9. The potential shifts are legal, i.e., each potential shift complies with various labor laws, and all its spells are time-compatible.

3.1.1. Design of the Nodes. Suppose T is the set of timetabled *trips*, D is the set of depots, and W is the set of feasible *spells*. We define two types of nodes.

(1) The depot node d, $d \in D$.

(2) The *spell node* w, $w \in W$. The *related nodes* for w represent one or more feasible *spell nodes* in the same *potential shift*.

Statement 10. Defining the shift as a node is infeasible.

If the *shifts* are defined as nodes, EVCSP can be illustrated in Figure 5. However, it is not feasible since the cost of the *shift* nodes needs to be defined in EVCSPM, which becomes a set partitioning CSP model and is incapable of handling EVSP.

3.1.2. Design of the Directed Arcs. Given the existence of two types of nodes, five directed arcs follow:

(1) A pull-out arc connects a depot to a *spell*.

(2) A pull-in arc connects a *spell* to a depot.

(3) A spell-link arc connects two *spells*.

(4) A recharge-link arc connects a *spell* to another *spell* through a hidden recharge point.

(5) A depot-return arc connects two *spells* with a temporary depot stop if the time gap between the consecutive *spells* is large enough (e.g., 3 h). An EV does not recharge in a depot-return arc.

The *spell* node consists of multiple *trips* connected by trip-link arcs. We define the trip-link arc as an implicit arc, while the pull-out, pull-in, spell-link, and recharge-link arcs are explicit.

A *spell* is feasible if all implicit arcs within it are time- and energy-compatible. An explicit arc is also feasible, provided that its compatibility is met (see Section 4.3 for the definition of arc compatibility).

3.1.3. Design of the Cost. We present the *arc cost* and *shift cost* below. The *arc cost* represents the connection cost between consecutive nodes, which comprises deadheading time, idle time, and recharge cost (if recharging is required). The *shift cost* includes the *trip* connection cost within each *spell* included in the *shift* and the total wage cost.

Specifically, the *arc cost* C_{ij} between *nodes* i and j is defined as follows:

$$C_{ij} = \begin{cases} \text{DH}_{ij}, & \text{if } (i, j) \text{ is a pull} - \text{out arc}, i \in D, j \in T, \\ \text{DH}_{ij}, & \text{if } (i, j) \text{ is a pull} - \text{in arc}, i \in T, j \in D, \\ \text{DH}_{ij} + \text{ID}_{ij}, & \text{if } (i, j) \text{ is a spell} - \text{link arc}, i, j \in T, \\ \text{DH}_{ir} + \text{DH}_{rj} + \text{ID}_{irj} + C_r, & \text{if } (i, j) \text{ is a recharge} - \text{link arc}, i, j \in T, r \in R, \\ \text{DH}_{id} + \text{DH}_{dj}, & \text{if } (i, j) \text{ is a depot} - \text{return arc}, i, j \in T, d \in D, \end{cases} \tag{6}$$

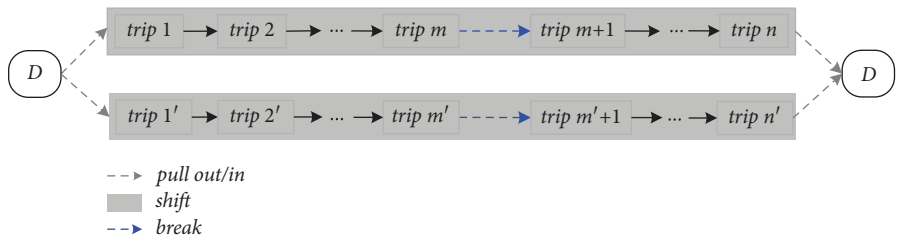

Figure 5: The *shift*-node-based network flow for the EVCSP.

where R denotes the set of recharge points and C_r represents the fixed recharge cost. DH_{ij} is the *deadheading time* between the arrival point of *trip i* and the departure point of *trip j*, DH_{ir} (DH_{id}) is the *deadheading time* between the arrival point of *trip i* and a recharge point r (depot d), DH_{rj} (DH_{dj}) is the *deadheading time* between a recharge point r (depot d) and the departure point of *trip j*, ID_{ij} stands for *idle time* for a spell-link arc (i, j), and ID_{irj} denotes the idle time for recharge-link arc(i, j). ID_{ij} and ID_{irj} are given as follows:

$$ID_{ij} = t_j^s - t_i^e - DH_{ij}, \tag{7}$$

$$ID_{irj} = t_j^s - t_i^e - DH_{ir} - DH_{rj} - T^{rt}, \tag{8}$$

where t_i^e represents the *end time* of *trip i*, t_j^s is the start *time* of *trip j*, and T^{rt} is the recharging time.

The *shift cost* C_s of *shift* s is defined as follows:

$$C_s = \sum_{t \in s} C_t + h(s), \tag{9}$$

where C_t represents the *trip* connection *cost* of *spell t* included in s, comprising the *idle time* and *deadheading time* between adjacent *trips*. The total wage cost of s is represented by $h(s)$.

For a viable integrated schedule, both C_{ij} and C_t constitute elements of the vehicle schedule cost, whereas $h(s)$ contributes to the crew schedule cost.

Statement 11. Adding the fixed trip cost to the arc and shift costs is unnecessary.

Since a feasible schedule must cover all the timetabled *trips*, the *trip cost* remains constant regardless of the selected schedule.

3.1.4. Constraints on the Paths. To satisfy the complex constraints associated with EVCSP for a chosen path, we impose the following constraints on the EV flow: constraint (1) ensures the path's integrity, while constraints (2) and (3) aim to create integrated schedules, $d_i, d_j \in D$.

(1) Each path must start from a source node d_i, followed by a sequence of feasible *nodes* connected by directed arcs, ending at a sink node d_j. $i = j$, when the path needs to return to the home depot

(2) Each node in a selected path can be covered by only one selected *shift*

(3) The selected paths and *shifts* should cover each timetabled trip precisely once

3.2. Compatibility of Arcs. Creating explicit arcs, including pull-out, pull-in, spell-link, and recharge-link arcs, is crucial to EVCSP, while forming implicit arcs, i.e., trip-link arcs, serves as the foundation for the *spell* node. An arc is present only if it satisfies both time and energy compatibility.

3.2.1. Time Compatibility. Two consecutive *trips*, i and j, within a *spell* are considered time-compatible if formula (1) is satisfied. This definition can be extended to spell link. Suppose the last *trip* in *spell p* is denoted as *trip i*, and the first *trip* in *spell q* is denoted as *trip j*. If formula (1) is met, the spell-link arc (p, q) is time-compatible. Similarly, the recharge-link arc (p, q) is time-compatible if formula (10) is satisfied

$$T_i^e + DH_{ir} + DH_{rj} \le T_j^s, \tag{10}$$

where DH_{ir} represents the *deadheading time* from the arrival point of *trip i* to the recharge point r and DH_{rj} denotes the *deadheading time* from r to the departure point of *trip j*.

3.2.2. Energy Compatibility. The energy consumption for executing *trip i* is denoted by e_i, and the EV energy left before serving *trip i* is denoted by e_i^s. If trip-link arc(i, j) exists and is selected in a *spell*, then $e_j^s = e_i^s - e_i - DE_{ij}$, where DE_{ij} represents the deadhead energy consumption from the arrival point of *trip i* to the departure point of *trip j*.

The energy consumption for executing *spell p* is denoted by E_p, and the EV energy left before serving *spell p* is E_p^s. The energy left after serving *spell p* is noted as E_p^e, which is equal to $E_p^s - E_p$. If a spell-link arc (p, q) exists and is selected, then $E_q^s = E_p^s - E_p - DE_{pq}$, where DE_{pq} signifies the deadhead energy consumption from the arrival point of the last *trip* in p to the departure point of the first *trip* in q.

We set a threshold, $E_{\min}$, to avoid EV breakdown during the *spell* (*trip*) serving. For two consecutive *trips*, i and j, in a *spell*, only those that are time-compatible can be evaluated for energy compatibility. The trip-link arc (i, j) exists if the following formula (11) is satisfied.

$$e_i^e - DE_{ij} - e_j - DE_{jr} \ge E_{\min} \left(i.e., e_j^e - DE_{jr} \ge E_{\min}\right), \tag{11}$$

where DE_{jr} is the deadhead energy consumption from the arrival point of *trip j* to r.

Similarly, for two *spells*, p and q, we can only discuss their energy compatibility if they are time-compatible. Let us assume that p and q are time-compatible for a trip link. The spell-link arc (p, q) exists if they are energy-compatible, which defined as

$$E_p^e - DE_{pq} - E_q - DE_{qr} \geq E_{\min} \left(\text{i.e., } E_q^e - DE_{qr} \geq E_{\min}\right), \tag{12}$$

where DE_{qr} is the deadhead energy consumption from the arrival point of the last *trip* in q to r. Assume that *spells* p and q are time-compatible for recharge link. If formula (12) is not fulfilled but conforms to formula (13) represented below, a recharge-link arc (p, q) exists

$$E_p^e - \text{DE}_{pr} \geq E_{\min}, \tag{13}$$

where DE_{qr} signifies the deadhead energy consumption from the arrival point of the last *trip* in q to r. In all cases, the EV can reach the recharging station before reaching $E_{\min}$.

3.3. Recharging and Discharging of EV Batteries. Given the limitation of EV battery capacity, it is crucial to develop effective recharging strategies and monitor the EV's energy consumption.

3.3.1. Energy Consumption of an EV. We calculate the energy consumption during the *trip* and deadhead while considering the states of prevailing driving and standstill.

Urban EVs in the bus market are generally required to operate at a relatively stable speed. Fontana [64] demonstrates that the net energy consumption linked to acceleration is almost zero along a specific path under certain simplifying assumptions. In calculating the prevailing driving energy consumption, we applied the following formula proposed by Fontana [64], which accounts for various factors, including air density, driving speed, air conditioning usage, and complex road surfaces.

$$f(v) = \frac{1}{\eta}\left(\frac{\rho C_\omega A_f v^2}{2} + \mu \text{mg}\cos\alpha + \text{mg}\sin\alpha\right) + \frac{P_{\text{acc}}}{v}. \tag{14}$$

The formula consistently measures the energy consumption per unit distance under the driving speed, $v\,(m/s)$. Within the formula, the symbol η represents the efficiency parameter, ρ (kg/m^3) is the air density, C_ω is the EV's drag coefficient, $A_f\,(m^2)$ refers to the frontal area, μ represents the friction coefficient, m (kg) is the EV's mass, $g\,(m/s^2)$ is the gravitational constant, and α(radians) measures the road angle, whereas $P_{\text{acc}}(W)$ represents the energy consumption used up by accessory loads, including air conditioners, headlights, and EV management systems.

Proposition 12. *EV's per-distance energy consumption* $f(v)$ *is minimized if* $v = \sqrt[3]{\eta P_{acc}/\rho C_\omega A_f}$.

Proof. Let $f'(v)$ be the first derivative of $f(v)$ with respect to v. $f'(v) = \rho C_\omega A_f v/\eta - P_{\text{acc}}/v^2$. If $f'(v) = 0$, $(\rho C_\omega A_f/\eta)v - P_{\text{acc}}/v^2 = 0$, $v = \sqrt[3]{\eta P_{\text{acc}}/\rho C_\omega A_f}$. If $v \in \left[0, \sqrt[3]{\eta P_{\text{acc}}/\rho C_\omega A_f}\right]$, $f'(v) < 0$, then $f(v)$ steadily decreases in the interval. If $v \in (\sqrt[3]{\eta P_{\text{acc}}/\rho C_\omega A_f}, +\infty)$, $f'(v) > 0$, then $f(v)$ steadily increasing. Therefore, $f(v)$ is minimized at $v = \sqrt[3]{\eta P_{\text{acc}}/\rho C_\omega A_f}$.

Tang et al. [70] set the parameters as $\rho = 1.2\,\text{kg/m}^3$, $C_\omega = 0.29$, $A_f = 2.27\,\text{m}^2$, $\eta = 0.9$, $g = 9.8 m/s^2$, $\alpha = 0$, and $\mu = 0.012$. The air conditioner consumes 7000 W of power P_{acc} if turned on and 2000 W otherwise. Let m_{EV} denote the weight of the EV, c_p denote the passenger capacity, and w_{avg} denote the average adult weight. Then, the total weight of the EV under the crew-only scenario is $m = m_{\text{EV}} + w_{\text{avg}}$, whereas the total weight under the fully loaded scenario is $m = m_{\text{EV}} + c_p w_{\text{avg}}$. Proposition 12 shows that in the absence of air conditioning, the function for the EV's energy consumption per unit distance $f(v)$ is minimized when $v = 13.16 m/s \approx 47 km/h$, while in the presence of air conditioning, it is minimized when $v = 19.98 m/s \approx 72 km/h$. However, in practice, the speed of EVs is often limited to 25~40 km/h for safety reasons. Therefore, we set $v = 40 km/h$.

The energy consumption of an EV during a standstill is approximately equal to P_{acc}.

Let D_i and D_{ij} be the fixed distances traveled for trip i and deadhead from i to j $(i, j \in T \cup D \cup R)$, respectively. The energy consumption e_i and e_{ij} for *trip* i and deadhead from i to j, respectively, can be calculated as follows:

$$\begin{aligned} e_i &= P_{\text{acc}} \times \left(T_i - \frac{D_i}{v}\right) + f(v)_{m=m_{\text{EV}}+c_p w_{\text{avg}}} \times D_i, \\ e_{ij} &= P_{\text{acc}} \times \left(\text{DH}_{ij} - \frac{D_{ij}}{v}\right) + f(v)_{m=m_{\text{EV}}+w_{\text{avg}}} \times D_{ij}, \end{aligned} \tag{15}$$

where T_i is the trip time taken for *trip* i. □

3.3.2. Recharging Strategy. We employ the current mainstream recharge strategy, which involves slow recharging at night and fast recharging during daily operations. Prior to initiating daily operations, the EVs undergo full charging.

For the recharge-link arc(p, q) to exist, *spells* p and q must be time-compatible for the recharge link, $E_p^e - \text{DE}_{pq} - E_q - \text{DE}_{qr} < E_{\min}$ and $E_p^e - \text{DE}_{pr} \geq E_{\min}$, which taking into consideration the EV energy left after serving *spell* p (E_p^e), the energy consumption of *spell* q (E_q), and the deadhead energy consumptions (DE_{pq}, DE_{qr}, and DE_{pr}).

Assuming the EV battery capacity is denoted as E_{full} (kW), the fast-recharge power as P_f (kW), and the recharge time as T^{rt} (min). Let the updated EV energy after recharging at recharge point r be denoted as E, which is given by

$$E = \begin{cases} E_p^e - \text{DE}_{pr} + P_f \cdot T^{rt}, & \text{if } E_p^e - \text{DE}_{pr} + P_f \cdot T^{rt} \leq E_{\text{full}}, \\ E_{\text{full}}, & \text{else.} \end{cases} \tag{16}$$

Thus, the EV energy left before serving *spell* q is $E_q^s = E - \text{DE}_{rq}$.

The determination of whether the connection arc between *spells* complies with the energy constraint cannot be made in advance. It can only be ascertained once the EV's completed *spells* are known during the scheduling process. This will indicate whether the EV can execute subsequent

spells using either the spell-link arc or the recharge-link arc. If the remaining energy of an EV cannot support the execution of a *spell* during the scheduling process, then the *spell* will not be considered for selection. However, the *spell* may still be selected if the EV goes to the recharge point for recharging, and the recharge link between the *spell* and the last *spell* currently selected by the EV is compatible in terms of time.

4. Integrated Model for Electric Vehicle and Crew Scheduling

As described in Section 3, the EVCSP involves identifying the optimal sequence of feasible nodes connected by directed arcs to cover all tasks at minimum cost. Each path must originate from and terminate at a node within the depot set D. The sequence of intermediate nodes must be feasible and connected by directed arcs. Table 2 lists the symbols used in EVCSPM, where $d_i, d_j \in D, w_i, w_j \in W$, and $t_i \in T$.

The EVCSPM is formulated below based on the expressions and symbols.

$$\textbf{(EVCSPM)} \quad \min \sum_{(d_i,w_j)\in PO} C_{d_i,w_j} x_{d_i,w_j} + \sum_{(w_i,w_j)\in SL\cup RL\cup DR} C_{w_i,w_j} x_{w_i,w_j} + \sum_{(w_i,d_j)\in PI} C_{w_i,d_j} x_{w_i,d_j} + \sum_{s\in S} C_s y_s, \tag{17}$$

$$\text{s.t} \sum_{w_j:(w_i,w_j)\in SL\cup RL\cup DR} x_{w_i,w_j} + \sum_{d_j:(w_i,d_j)\in PI} x_{w_i,d_j} = \sum_{s\in S} \lambda_s^{w_i} y_s, \quad \forall w_i \in W, \tag{18}$$

$$\sum_{w_j:(w_j,w_i)\in \mathrm{SL}\cup \mathrm{RL}\cup \mathrm{DR}} x_{w_j,w_i} + \sum_{d_j:(d_j,w_i)\in \mathrm{PO}} x_{d_j,w_i} = \sum_{s\in S} \lambda_s^{w_i} y_s, \quad \forall w_i \in W, \tag{19}$$

$$\sum_{s\in S} \lambda_s^{w_i} y_s \le 1, \quad \forall w_i \in W, \tag{20}$$

$$\sum_{w_j:(d_i,w_j)\in \mathrm{PO}} x_{d_i,w_j} - \sum_{w_k:(w_k,d_i)\in \mathrm{PI}} x_{w_k,d_i} = 0, \quad \forall d_i \in D, \tag{21}$$

$$\sum_{s\in S} \gamma_s^{t_i} y_s = 1, \quad \forall t_i \in T, \tag{22}$$

$$\begin{aligned} E_{w_j}^e = {} & \sum_{d_i:(d_i,w_j)\in \mathrm{PO}} \left(E_{\mathrm{full}} - \mathrm{DE}_{d_i,w_j} - E_j\right) \cdot x_{d_i,w_j} + \sum_{w_i:(w_i,w_j)\in \mathrm{SL}} \left(E_{w_i}^e - \mathrm{DE}_{w_i,w_j} - E_j\right) \cdot x_{w_i,w_j} \\ & + \sum_{w_i:(w_i,w_j)\in \mathrm{RL}} \min\left\{E_{\mathrm{full}} - \mathrm{DE}_{r,w_j} - E_j, E_{w_i}^e - \mathrm{DE}_{w_i,r} + P_f \cdot T^{rt} - \mathrm{DE}_{r,w_j} - E_j\right\} \cdot x_{w_i,w_j} \\ & + \sum_{w_i:(w_i,w_j)\in \mathrm{DR}} \left(E_{w_i}^e - \mathrm{DE}_{w_i,d_k} - \mathrm{DE}_{d_k,w_i} - E_j\right) \cdot x_{w_i,w_j}, \quad \forall w_j \in W, d_k \in D, \end{aligned} \tag{23}$$

$$E_{w_i}^e \ge E_{\min} + DE_{w_i,r}, \text{if} \sum_{d_j:(d_j,w_i)\in \mathrm{PO}} x_{d_j,w_i} + \sum_{w_j:(w_j,w_i)\in \mathrm{SL}\cup \mathrm{RL}\cup \mathrm{DR}} x_{w_j,w_i} > 0, \quad \forall w_i \in W, \tag{24}$$

$$y_s \in \{0,1\}, \quad \forall s \in S, \tag{25}$$

$$x_{w_i,w_j} \in \{0,1\}, \quad \forall (w_i,w_j) \in \mathrm{SL}\cup \mathrm{RL}\cup \mathrm{DR}, \tag{26}$$

$$x_{d_i,w_j} \in \{0,1\}, \quad \forall (d_i,w_j) \in \mathrm{PO}, \tag{27}$$

$$x_{w_i,d_j} \in \{0,1\}, \quad \forall (w_i,d_j) \in \mathrm{PI}. \tag{28}$$

Table 2: Sets, parameters, and variables of the EVCSPM.

Sets	
T	Set of timetabled *trips*
S	Set of *shifts*
W	Set of *spells*
D	Set of depots
PO	Set of pull-out arcs
PI	Set of pull-in arcs
SL	Set of spell-link arc
RL	Set of recharge-link arc
DR	Set of depot-return arcs
A	Set of arcs A = PO ∪ PI ∪ SL ∪ RL ∪ DR
Parameters	
C_s	*Cost* of the *shift* s
C_{d_i,w_j}	*Arc cost* from d_i to w_j
C_{w_i,w_j}	*Arc cost* from w_i to w_j
C_{w_i,d_j}	*Arc cost* from w_i to d_j
T^{rt}	Recharge time
P_f	Fast-recharge power
$E_{\min}$	Energy threshold
E_j	Energy consumption of w_j
E_{d_i,w_j}	Energy consumption from d_i to w_j
E_{full}	Total EV battery capacity
DE_{w_i,w_j}	Deadhead energy consumption from w_i to w_j
DE_{r,w_j}	Deadhead energy consumption from r to w_j
$\text{DE}_{w_i,r}$	Deadhead energy consumption from w_i to r
Variables	
$x_{w_i.w_j}$	=1, if the arc from w_i to w_j is selected; =0, otherwise
$x_{d_i.w_j}$	=1, if the arc from d_i to w_j is selected; =0, otherwise
$x_{w_i.d_j}$	=1, if the arc from w_i to d_j is selected; =0, otherwise
y_s	=1, if *shift* s is selected; =0, otherwise
$E^e_{w_i}$	EV energy left after serving w_i
Others	
$\lambda_s^{w_i}$	=1, if *shift* s contains *spell* w_i; =0, otherwise
$\gamma_s^{t_i}$	=1, if *shift* s contains *trip* t_i; =0, otherwise

The decision variable x_{ij} takes a value of 1 if the arc (i, j) is selected. Similarly, y_s takes a value of 1 if the *shift* s is selected and 0 otherwise. Formula (17) aims to minimize the total cost comprising operating and wage costs. This is achieved through the cost definitions in formulas (6)–(9). Formulas (18)–(20) represent the conservation of flows, which ensures that each selected *spell* node is covered by only one EV. Formula (21) represents the conservation of depots, which ensures an equal fleet size to pull-out from and pull-in to a depot. Formula (22) represents the constraint of *trips*, which ensures that each *trip* is covered by only one crew. Formula (23) represents the energy state transition of EVs. Formula (24) represents the remaining energy constraint of EVs, which must always be kept above $E_{\min}$. Finally, formulas (25)–(28) represent the value constraints of the decision variables. We have assessed the feasibility of the EVCSPM by solving an instance for which the optimal schedule is known in advance, using the GUROBI solver.

Table 3: The number of variables and constraints for the EVCSP models.

Models	Variables	Constraints
EVCSPM	$q^2 + 2pq + m$	$5q + p + n$
EVCSPM-1	$r + m$	$n^2 + 2n$
EVCSPM-2	$n^2 + m + 4n$	$2n^2 + 13n$

Research on EVCSP is extremely limited. Our model's complexity is compared to the only two EVCSP models, EVCSPM-1 [7] and EVCSPM-2 [34], using two indicators: the number of variables and constraints. Table 3 displays the results, where B represents the set of blocks and S represents the set of *shifts*, $|D| = p, |W| = q, |S| = m, |T| = n, |B| = r$.

In Table 3, the inequality $n^2 + m + 4n < 2pq + q^2 + m << r + m$ holds. The EVCSPM-2 has the fewest decision variables compared to other models, while the EVCSPM model maintains a reasonable number of variables. In practice, the feasibility of *spells* is restricted by various labor regulations. Consequently, $5q + p + n << n^2 + 2n < 2n + n^2$. As a result, the EVCSPM imposes the fewest constraints. Overall, the EVCSPM demonstrates a low level of complexity.

Efficient resource utilization is the main objective of scheduling.

Statement 13. To limit the fleet and crew size, substitute formula (17) with (29), where C_{veh} and C_{crew} refer to the fixed cost of EV and crew, respectively, while $\alpha, \beta \in (0, +\infty)$ represent adjustment parameters.

$$\sum_{(d_i,w_j)\in \text{PO}} \left(C_{d_i,w_j} + \alpha C_{\text{veh}}\right) x_{d_i,w_j} + \sum_{(w_i,w_j)\in \text{SL}\cup\text{RL}\cup\text{DR}} C_{w_i,w_j} x_{w_i,w_j} + \sum_{(w_i,d_j)\in \text{PI}} C_{w_i,d_j} x_{w_i,d_j} + \sum_{s\in S} (C_s + \beta C_{\text{crew}}) y_s. \tag{29}$$

Choosing a pull-out arc represents selecting an empty EV that must be utilized. Consequently, if a pull-out arc is chosen as part of the path, a significant enough cost of αC_{veh} is added as a penalty that could reduce the fleet size. Similarly, selecting a *shift* s requires a crew to be available. Therefore, if a *shift* s is chosen as part of the path, a cost of βC_{crew} is added as a penalty that could reduce the crew size.

Typically, an EV requires depart from and return to the same depot.

Statement 14. Assuming that each path must cover a maximum of two spells (constrained by formula (30)), the subsequent formula (31) ensures that the path returns to the home depot.

$$\sum_{w_l:(w_l,w_i)\in \mathrm{SL}\cup \mathrm{RL}\cup \mathrm{DR}} x_{w_l,w_i} = \sum_{w_k:(w_j,w_k)\in \mathrm{SL}\cup \mathrm{RL}\cup \mathrm{DR}} x_{w_j,w_k} = 0, \quad \forall x_{w_i,w_j} = 1, \tag{30}$$

$$x_{d_k,w_i} - x_{w_j,d_k} = 0, \forall x_{w_i,w_j} = 1, d_k \in D. \tag{31}$$

5. Solution Method

This section proposes a hybrid approach for the EVCSP that integrates both the heuristic method and ILP. The fundamental approach is compiling the *potential shifts* using a matching-based heuristic and subsequently solving EVCSP iteratively with an ILP solver named GUROBI.

The heuristic method, employing a matching-based approach, generates *shift* set to comply with a range of labor regulations and restrains the crew size through a set of "soft constraints" represented as filter conditions. The heuristic methodology comprises three steps: tier-partitioning, spell-constructing, and shift-generating. Algorithm 1 of the tier-partitioning step splits the timetabled *trips* $T = \{1, 2, \ldots, n\}$ into several nonoverlapping *incompatible sets* labeled as $S_0, S_1, \ldots, S_K$, with T arranged in ascending order by departure time. Here, $S_i = \{j | j \epsilon T \ \& \ tier(j) = i\}$, with $tier(j)$ representing the tier number for *trip* j, $i = 0, 1, \ldots, K$.

We construct the *spells* with partitioned *trip* tiers $S_0, S_1, \ldots, S_K$. However, generating all feasible *spells* can be challenging when solving realistic EVCSP. Thus, to address this issue, we use Algorithm 2 to find the *spells* led by each trip of each tier in turn. Specifically, the algorithm applies the following restrictions: (1) the *spell* comprises l *pieces* (*spell_l*) where the linking arcs are the edges of the maximum cardinality matching between adjacent tiers, $p \le l \le q$, and (2) the feasible length of the *spell* is limited to [*len_Min*, *len_Max*], as specified in labor regulations. Here, *spell_S* represents the set of *spells*, and *len_spell* corresponds to the *spell*'s length, defined as the time interval between the end time of the preceding *trip* and the start time of the initial *trip* within the *shift*.

The shift-generating Algorithm 3 generates *shift* set referred to as *PS*. Considering labor regulations, Algorithm 3 restraints the minimum and maximum break and work times. Here, *break_MinStr* and *break_MaxStr* denote the minimum and maximum break times, respectively. Similarly, *work_Min* and *work_Max* represent the minimum and maximum work times, where the work duration is calculated as the difference between the *shift*'s time span and the break time. sT_i and eT_i signify the start and end times of $spell_i$, and the tw_{ij} indicates the work time of a straight *shift* (i, j).

Each straight *shift* generated by Algorithm 3 consists of two *spells*. *PS* is constructed to include all *tripper shifts* to ensure that they cover all timetabled *trips*. Each tripper *shift* in *PS* only comprises one *spell*. The schedule-producing Algorithm 4 updates the optimal integrated schedule by circularly solving the EVCSP subproblem, where F represents the iteration threshold, *#shift* represents the number of *shifts*, and EVCSP_*shift_S*′ is the EVCSP with the *potential shifts* set *shift_S*′.

The framework of the hybrid approach is illustrated in Figure 6, where T is the timetabled *trips*.

6. Experiments and Results

A series of experiments are conducted based on a case study of bus route 2 in Xiaogan, Hubei, China (XGR2), which operates pure EVs. The XGR2 route spans 12.7 km and has 30 stops, servicing 270 *trips* daily. The EVs maintain a consistent departure interval of 5~8 min throughout the day. The EVs used are of the pure EV type XML6105, with a weight of 11,000 kg, rated capacity for 40 passengers, and battery capacity of 140 kWh. The average weight of an adult passenger is 62 kg. The fast- and slow-recharge power is 160 kW and 60 kW, respectively. We obtain eight variant instances (T1~T8) from XGR2 to test our method and model. The distribution of timetabled trips for each instance is illustrated in Figure 7.

In Section 6.1, we implement orthogonal experiments to determine the optimal parameter settings for our hybrid heuristic method and EVCSPM. In Section 6.2, we compare our method with GUROBI via comparative experiments. Subsequently, we test the performance of EVCSPM versus the sequential model in Section 6.3. Lastly, we conduct a sensitivity analysis on the parameters in Section 6.4.

6.1. Experiments for Optimal Parameter Settings. Table 4 displays the guidelines for work assignments for various *shift* types in the test instances. *#spell* indicates the number of *spells*. A 1-*spell shift* unequivocally consists of only one *spell*, whereas a 2-*spell shift* includes two consecutive *spells* with an intervening break.

We assigned a cost of 1,000 for the utilization of each EV or crew, denoted as $C_{\mathrm{veh}} = C_{\mathrm{crew}} = 1{,}000$. Additionally, there is a small variable cost of 1 for every minute an EV operates outside the depot and a cost of 0.1 for each minute, the crew works. The fixed recharge cost, C_r, is set at 15, recharge time T^{rt} at 30 min, and energy threshold $E_{\min}$ at 10 kW. EVCSPM

(1) $T \longleftarrow \{1,2,3, \ldots, n\}$, {tier(1), tier(2), . . ., tier(n)} $\longleftarrow$ {0, 0, . . ., 0), $i \longleftarrow 1$
(2) **while** $i < n+1$ **do**
(3) $j \longleftarrow i+1$
(4) **while** $j < n+1$ **do**
(5) **if** $i\Theta j$ or $i\Theta j$ **then** tier(j) = tier(i) + 1
(6) $j \longleftarrow j+1$
(7) **end while**
(8) $i = i+1$
(9) **end while**
(10) **return** {tier(1), tier(2), . . ., tier(n)}

Algorithm 1: Tier-partitioning.

(1) $S_0, S_1, \ldots, S_K$, $spell\_S \longleftarrow \varnothing, t \longleftarrow 0, l \longleftarrow 0$
(2) **while** $t < K$ **do**
(3) maximum cardinality matching for S_t and S_{t+1}
(4) $t \longleftarrow t+1$
(5) **end while**
(6) $t \longleftarrow 0$
(7) **while** $t < K$ **do**
(8) **for** each $j \epsilon S_t$ **do**
(9) select the matched edges to construct all executable *spells* led by j
(10) **if** $len\_Min \le len\_spell \le len\_Max$ && $p \le l \le q$ **then** $spell\_S \longleftarrow spell\_S \cup \{spell\}$
(11) **end for**
(12) $t = t+1$
(13) **end while**
(14) **return** *spell_S*

Algorithm 2: Spell-constructing.

(1) $spell\_S, nS \longleftarrow |spell\_S|$, $PS \longleftarrow \varnothing, i \longleftarrow 1$
(2) **while** $i < nS$ **do**
(3) $j \longleftarrow i+1$
(4) **while** $j < nS+1$ **do**
(5) $t_{ij} \longleftarrow sT_j - eT_i$
(6) **if** $break\_MinStr \le t_{ij} \le break\_MaxStr$, $work\_Min \le tw_{ij} \le work\_Max$, & $ValidStraight\ (i, j) == \text{TRUE}$
(7) **then** PS $\longleftarrow$ PS$\cup$Straight (i, j)
(8) $j \longleftarrow j+1$
(9) **end while**
(10) **end while**
(11) **return** *PS*

Algorithm 3: Shift-generating.

relies on four crucial parameters: coefficients α and β in equation (29), and p and q in Algorithm 2 line 10. We use the Taguchi orthogonal method with orthogonal table $L_9(3^4)$ to evaluate the most appropriate parameter settings. The selected levels are shown in Table 5. We ran tests on T1 and T2 to evaluate the performance. Table 6 lists the test results, with cost representing the total operating cost of the EV and the crew working time.

Based on Table 6, the range analysis results are shown in Table 7, where R_f, R_{cr}, R_{fcr}, and R_c are the extremum differences (EDs) corresponding to the fleet size, crew size, fleet and crew size, and cost, respectively.

Table 7 indicates the minimum fleet sizes for T1 in terms of α, β, p, and q are $\overline{f_{1\alpha}} = \overline{f_{2\alpha}} = \overline{f_{3\alpha}} = 19.3$, $\overline{f_{1\beta}} = \overline{f_{2\beta}} = \overline{f_{3\beta}} = 19.33$, $\overline{f_{1p}} = \overline{f_{2p}} = 19$, and $\overline{f_{1q}} = \overline{f_{2q}} = 19$,

(1) PS, $i \longleftarrow 1$, F, n, $SC \longleftarrow \varnothing$
(2) **while** $i < F$ **do**
(3) call GUROBI to find a minimal *#shift* crew schedule *shift_S* for the CSP with PS as the *potential shifts*
(4) randomly selecting n *shifts* from PS and incorporating them into *shift_S* to create $shift\_S'$
(5) call GUROBI to find an integrated schedule SC' for the $EVCSP\_shift\_S'$
(6) **if** $fit(SC) > fit(SC')$
(7) **then** $SC \longleftarrow SC'$
(8) aim at the *blocks* in SC', construct a new *shift* set to extend to PS
(9) $i \longleftarrow i + 1$
(10) end while
(11) **return** SC

Algorithm 4: Schedule-producing.

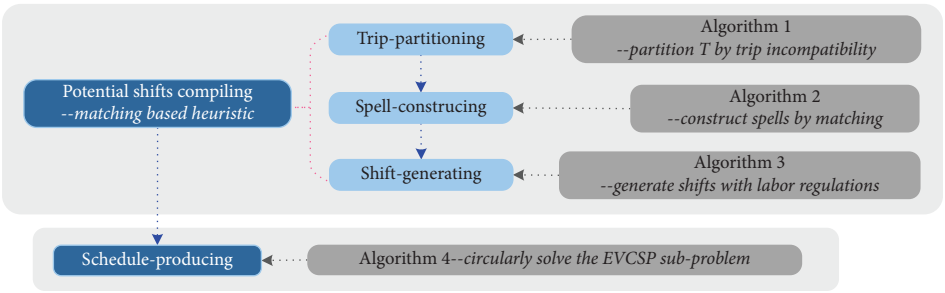

Figure 6: The framework of the hybrid heuristic.

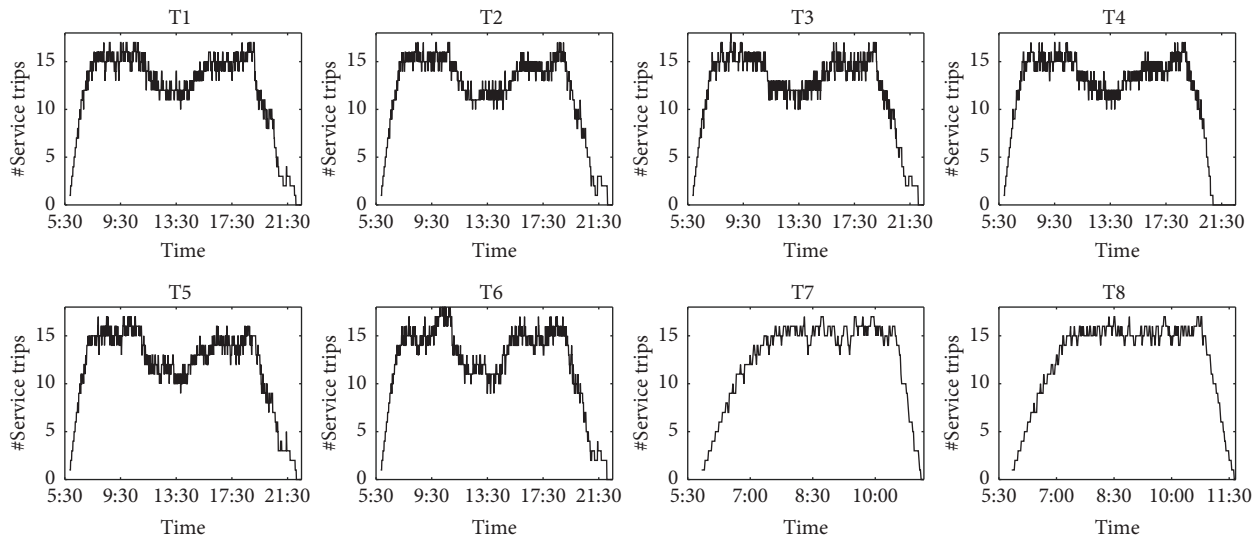

Figure 7: Distribution of service trips over the day for instances T1~T8. #service trips are the number of simultaneous service trips.

Table 4: Work rules for 1-*spell* and 2-*spell shifts*.

	1-*spell*		2-*spell*	
	Minimum	Maximum	Minimum	Maximum
#spell	1	1	2	2
Shift length	45	270	45	540
Spell	45	270	45	270
Break time	0	0	30	60
Work time	45	270	45	450

Table 5: Three levels for each of the three factors.

Levels	α	β	p	q
1	1	1	1	4
2	2	2	2	5
3	3	3	3	6

Table 6: Results of the orthogonal test proposed by the hybrid heuristic method on solving EVCSPM for optimal parameter settings (instances: T1~T2).

No.	α	β	p	q	Fleet size		Crew size		Fleet + crew size		Cost	
					T1	T2	T1	T2	T1	T2	T1	T2
1	1	1	1	1	19	19	40	38	59	57	4736	4858
2	1	2	2	2	19	18	39	37	58	55	4281	4213
3	1	3	3	3	20	23	40	42	60	65	4437	4146
4	2	1	2	3	19	18	39	37	58	55	4251	4231
5	2	2	3	1	20	23	43	45	63	68	4714	4514
6	2	3	1	2	19	18	39	37	58	55	4281	4213
7	3	1	3	2	20	23	41	42	61	65	4200	4128
8	3	2	1	3	19	18	39	37	58	55	4251	4231
9	3	3	2	1	19	19	40	38	59	57	4736	4858

Table 7: Results of the range analysis for optimal parameter settings (instances: T1~T2).

Item	ED	T1				T2			
		α	β	p	q	α	β	p	q
Fleet size	f_1	58	58	57	58	60	60	55	61
	f_2	58	58	57	58	59	59	59	59
	f_3	58	58	60	58	60	60	69	59
	$\overline{f_1}$	19.3	19.3	19	19	20	20	18.3	20.3
	$\overline{f_2}$	19.3	19.3	19	19	19.7	19.7	19.7	19.7
	$\overline{f_3}$	19.3	19.3	20	20	20	20	23	19.7
	R_f	0	0	1	1	0.3	0.3	4.7	0.6
Crew size	cr_1	119	120	118	123	117	117	112	121
	cr_2	121	121	118	119	119	119	112	116
	cr_3	120	119	124	118	117	117	129	116
	$\overline{cr_1}$	39.7	40	39.3	41	39	39	37.3	40.3
	$\overline{cr_2}$	40.3	40.3	39.3	39.7	39.7	39.7	37.3	38.7
	$\overline{cr_3}$	40	39.7	41.3	39.3	39	39	43	38.7
	R_{cr}	0.6	0.6	2	1.7	0.7	0.7	5.7	1.6
Fleet + crew size	fcr_1	177	178	175	181	177	177	167	182
	fcr_2	179	179	175	177	178	178	171	175
	fcr_3	178	177	184	176	177	177	198	175
	$\overline{fcr_1}$	59	59.3	58.3	60.3	59	59	55.7	60.7
	$\overline{fcr_2}$	59.7	59.7	58.3	59	59.3	59.3	57	58.3
	$\overline{fcr_3}$	59.3	59	61.3	58.7	59	59	66	58.3
	R_{fcr}	0.7	0.7	3	1.6	0.3	0.3	10.3	2.4
Cost	c_1	13454	13187	13268	14186	13217	13217	13302	14230
	c_2	13246	13246	13268	12762	12958	12958	13302	12554
	c_3	13187	14354	13351	12939	13217	13217	12788	12608
	$\overline{c_1}$	4484.7	4395.7	4422.7	4728.7	4405.7	4405.7	4434	4743.3
	$\overline{c_2}$	4415.3	4415.3	4422.7	4254	4319.3	4319.3	4434	4184.7
	$\overline{c_3}$	4395.7	4484.7	4450.3	4313	4405.7	4405.7	4262.7	4202.7
	R_c	89	89	7.6	474.7	86.4	86.4	171.3	558.6

respectively, and the minimum fleet sizes for T2 are $\overline{f_{2\alpha}} = 19.7$, $\overline{f_{2\beta}} = 19.7$, $\overline{f_{1p}} = 18.3$, and $\overline{f_{2q}} = \overline{f_{3q}} = 19.7$, respectively. The optimal combination for fleet size is $\alpha_2\beta_2p_1q_2$. The EDs hold $R_{fp} \geq R_{fq} > R_{f\alpha} = R_{f\beta}$. Accordingly, p has the most significant effect on fleet size. Similarly, the optimal combination for crew size is $\alpha_1\beta_3p_1$ (or p_2) q_3. The

parameters affect crew size in order: (main) $p \longrightarrow q \longrightarrow \alpha(\beta)$ (minor). The optimal combination for fleet + crew size is $\alpha_3\beta_1p_1q_3$. The parameters affect the fleet + crew size in order: (main) $p \longrightarrow q \longrightarrow \alpha(\beta)$ (minor). The optimal combination for the cost of T1 is $\alpha_3\beta_1p_1$ (or p_2) q_2, while that of T2 is $\alpha_2\beta_2p_3q_2$. The parameters affect the cost in order: (main) $q \longrightarrow p \longrightarrow \alpha$ (β) (minor). Prioritizing the minimization of fleet + crew size, it is evident that p_1(or p_2) q_3 is the most competitive option. α and β have a marginal influence on all four items. Thus, we select α_2 and β_2 based on their higher frequency of occurrence. The optimal factor level is $\alpha_2\beta_2p_2q_3$, which implies $\alpha = 2$, $\beta = 2$, $p = 2$, and $q = 6$.

6.2. Experiments on Hybrid Heuristic Method and GUROBI. This section aims to verify the effectiveness of the proposed heuristic method by comparing it to GUROBI using problems T1~T8. GUROBI solves the EVCSP with *PS* generated by Algorithms 1–3 as the *potential shifts*. The results are presented in Table 8, where #recharge refers to the number of recharges and the relative percentage deviations (RPDs) over the schedule produced by GUROBI are provided.

Table 8 shows that GUROBI cannot solve problems T1~T6. The sizes of the fleet and crew and the number of recharges generated by the hybrid heuristic method for T7 and T8 are the same as those produced by GUROBI. The average RPD in terms of cost for T7 and T8 is only 0.3%, but the average time taken by the heuristic method is only one-sixth of GUROBI's. Therefore, we employ this method, as the results produced are sufficiently good and efficient to evaluate EVCSPM.

6.3. Experiments on EVCSPM and Two-Stage Sequential Model. The section compares the proposed EVCSPM with the two-stage sequential model (TSM). TSM comprises the EVSP model, followed by the CSP model. We formulate the EVSP model by incorporating EV energy state transfer and energy threshold constraints into the traditional VSP model [71]. We adopt the classic set covering model [65] for crew scheduling.

Ideally, the same algorithm should be used to evaluate the performance of both models, but our heuristic method is tailored to EVCSPM and not easily adaptable to TSM. To ensure fairness to TSM, we solve it by sequentially processing the EVSP and CSP models with GUROBI. Moreover, because of the NP-hard property of EVCSPM and the limitations imposed by GUROBI's problem-solving capabilities, the energy constraint of EVSP is disregarded during the scheduling process for TSM. As a result, TSM can only provide a lower bound for EVSP's optimal EV schedule. We enumerate all feasible spells with the generated EV schedule and then generate *potential shifts* for the succeeding CSP model using Algorithm 3.

The comparison of schedules for problems T1~T8 is conducted using EVCSPM with the heuristic approach and TSM with GUROBI. Table 9 presents the relevant data on the number of tiers for timetabled *trips* and the resulting *spells* and *shifts* for both models. Specifically, *#tier* indicates the count of tiers, while *#spell_i* ($i = 2, 3, 4, 5, 6$) signifies the count of *spell_i*. The counts of *spells* (*#spell*) and *shifts* (*#shift*) overall are also included in the table. Table 10 presents additional details on the resulting schedules for both models. The RPDs, computed over the schedule proposed by TSM, are also included.

Table 9 shows that EVCSPM produces an average of 2322.75 *spells* and 132599.75 *shifts*, while TSM generates an average of 654.5 *spells* and 13696.63 *shifts*. The *potential shifts* generated by TSM are only one-tenth of those generated by EVCSPM. This difference may be explained by the obtained EV schedule limiting the construction of TSM's *potential shifts*. The results in Table 10 indicate that EVCSPM and TSM exhibit similar performance in terms of the number of recharges. Both models propose schedules with the same fleet size for problems T1~T2 and T4~T8. However, for T3, the schedule obtained by EVCSPM has a fleet size of three greater than that of TSM. Overall, TSM outperforms EVCSPM in terms of fleet size. For crew size, both models propose schedules with the same crew size for problems T7-T8. However, for problems T1–T6, EVCSPM outperforms TSM regarding crew size, with RPDs ranging from −2.5% to −5.1%. Regarding fleet + crew size, the schedule obtained by EVCSPM surpasses TSM only for T3, with a positive RPD of 3.6%, while the average RPD is −1.3%. EVCSPM also outperforms TSM in terms of fleet + crew size. For cost, EVCSPM outperforms TSM in terms of cost only for T6, with a positive RPD of 3.4%. However, the average RPD for cost is −8.7%. Finally, the average elapsed time for solving EVCSPM is 96.78s, while TSM requires 2371.75s, even without considering the energy constraint. Therefore, EVCSPM outperforms TSM regarding crew size, fleet + crew size, cost, and elapsed time.

To gain a deeper understanding of the performance of EVCSPM and TSM, we illustrate the schedules pertaining to fleet size, crew size, fleet + crew size, and cost in Figure 8.

The results illustrated in Figure 8 indicate EVCSPM's superior performance across the three subgraphs, except subgraph (a), as evidenced by the positioning of the EVCSPM polylines below corresponding TSM polylines. It has been confirmed that, in terms of crew size, fleet + crew size, and cost, EVCSPM outperforms TSM. Given the priority of minimizing fleet and crew size, we assert that EVCSPM is generally superior to TSM in EV and crew scheduling.

6.4. Sensitivity Analysis. This section conducts a sensitivity analysis of EVCSPM by examining the impact of critical parameters on fleet size, crew size, number of EV recharges, and cost. Specifically, we investigate the effects of battery capacity E_{full}, recharging time, and recharging power in equation (16) on these performances while considering the influence of coefficients α and β in equation (29). The aim is to provide a comprehensive understanding of the sensitivity of the EVCSPM model.

Table 8: Experimental results of EVCSPM produced by GUROBI and the hybrid heuristic method (T1~T8).

Problem	#trip	Method	Item					
			Fleet size	Crew size	Fleet + crew size	Cost	#recharge	Elapse time (s)
T1	279	GUROBI	—	—	—	—	—	—
		Heuristic	19	39	58	4308	5	81.33
		RPD	—	—	—	—	—	—
T2	273	GUROBI	—	—	—	—	—	—
		Heuristic	18	37	55	4143	4	233.51
		RPD	—	—	—	—	—	—
T3	279	GUROBI	—	—	—	—	—	—
		Heuristic	21	37	58	4422.3	5	157.93
		RPD	—	—	—	—	—	—
T4	280	GUROBI	—	—	—	—	—	—
		Heuristic	18	37	55	4272.5	5	77.37
		RPD	—	—	—	—	—	—
T5	270	GUROBI	—	—	—	—	—	—
		Heuristic	18	37	55	4133.5	5	75.2
		RPD	—	—	—	—	—	—
T6	280	GUROBI	—	—	—	—	—	—
		Heuristic	19	38	57	4376.7	6	102.51
		RPD	—	—	—	—	—	—
T7	60	GUROBI	17	17	34	666.4	0	1520.9
		Heuristic	17	17	34	681.3	0	21.7
		RPD	0%	0%	0%	2.2%	0%	—
T8	60	GUROBI	17	17	34	536	0	1247.1
		Heuristic	17	17	34	552.7	0	24.67
		RPD	0%	0%	0%	3.1%	0%	—
Avg. (T7~T8)	222.63	GUROBI	17	17	34	601.2	0	1384
		Heuristic	17	17	34	617	0	23.19
		RPD	0%	0%	0%	2.6%	0%	—

Table 9: Spells and potential shifts of EVCSPM and two-stage sequential models.

Problem	Model	Item							
		#tier	*#spell*	*#spell_2*	*#spell_3*	*#spell_4*	*#spell_5*	*#spell_6*	*#shift*
T1	EVCSPM	19	2457	357	474	630	768	228	117979
	TSM	—	820	260	241	211	99	9	17185
T2	EVCSPM	19	4698	505	697	928	1136	1432	307850
	TSM	—	826	255	237	212	114	8	17215
T3	EVCSPM	19	2813	482	608	771	779	173	171998
	TSM	—	882	261	241	219	128	33	20028
T4	EVCSPM	19	2402	356	460	605	705	276	118834
	TSM	—	885	262	244	222	133	24	20084
T5	EVCSPM	20	2822	361	512	732	962	255	157576
	TSM	—	821	252	234	211	110	14	16990
T6	EVCSPM	19	3078	377	521	750	1007	423	186162
	TSM	—	841	260	240	211	109	21	17888
T7	EVCSPM	4	158	76	70	12	0	0	179
	TSM	—	79	43	26	10	0	0	89
T8	EVCSPM	4	154	75	65	13	1	0	220
	TSM	—	82	43	26	12	1	0	94
Avg.	EVCSPM	15.38	2322.75	323.63	425.88	555.13	669.75	348.38	132599.75
	TSM	—	654.5	204.5	186.13	163.5	86.75	13.63	13696.63

Table 10: Schedules generated by EVCSPM and two-stage sequential models.

Problem	Model	Item					
		Fleet size	Crew size	Fleet + crew size	Cost	#recharge	Elapse time (s)
T1	EVCSPM	19	39	58	4308	5	81.33
	TSM	19	40	59	4638.3	5	55.7
	RPD	0%	−2.5%	−1.7%	−7.1%	0%	—
T2	EVCSPM	18	37	55	4143	4	233.51
	TSM	18	39	57	4469.7	4	3027.37
	RPD	0%	−5.1%	−3.5%	−7.3%	0%	—
T3	EVCSPM	21	37	58	4422.3	5	157.93
	TSM	18	38	56	4660.1	5	21.51
	RPD	16.7%	−2.6%	3.6%	−5.1%	0%	—
T4	EVCSPM	18	37	55	4272.5	5	77.37
	TSM	18	39	57	4343.4	5	6859.42
	RPD	0%	−5.1%	−3.5%	−1.6%	0%	—
T5	EVCSPM	18	37	55	4133.5	5	75.2
	TSM	18	38	56	4358.7	5	82.31
	RPD	0%	−2.6%	−1.8%	−5.2%	0%	—
T6	EVCSPM	19	38	57	4376.7	6	102.51
	TSM	19	40	59	4233.9	6	8856.52
	RPD	0%	−5%	−3.4%	3.4%	0%	—
T7	EVCSPM	17	17	34	666.4	0	21.7
	TSM	17	17	34	882.8	0	30.65
	RPD	0%	0%	0%	−24.5%	0%	—
T8	EVCSPM	17	17	34	536	0	24.67
	TSM	17	17	34	692	0	40.53
	RPD	0%	0%	0%	−22.5%	0%	—
Avg. (T7~T8)	EVCSPM	18.38	32.38	50.75	3357.3	0	96.78
	TSM	18	33.5	51.5	3534.86	0	2371.75
	RPD	2.1%	−2.9%	−1.3%	−8.7%	0%	—

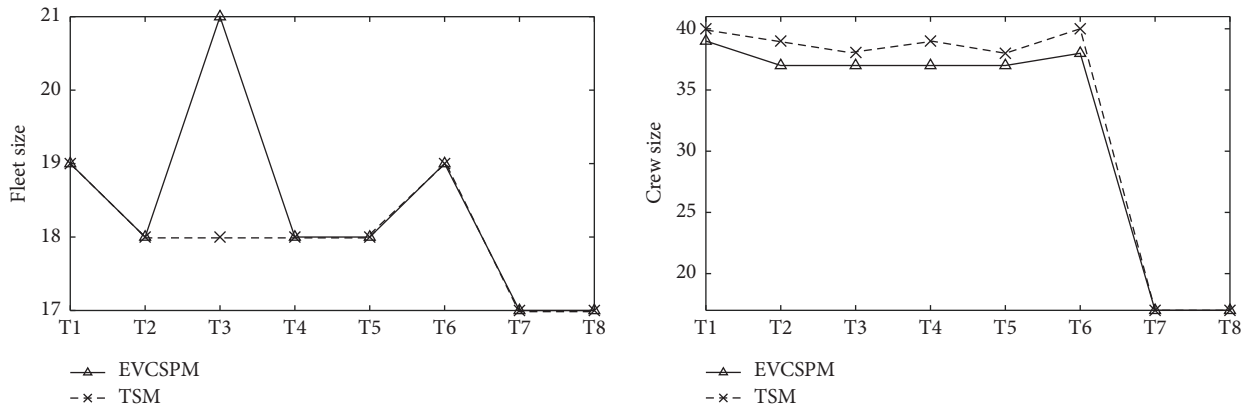

(a) (b)

Figure 8: Continued.

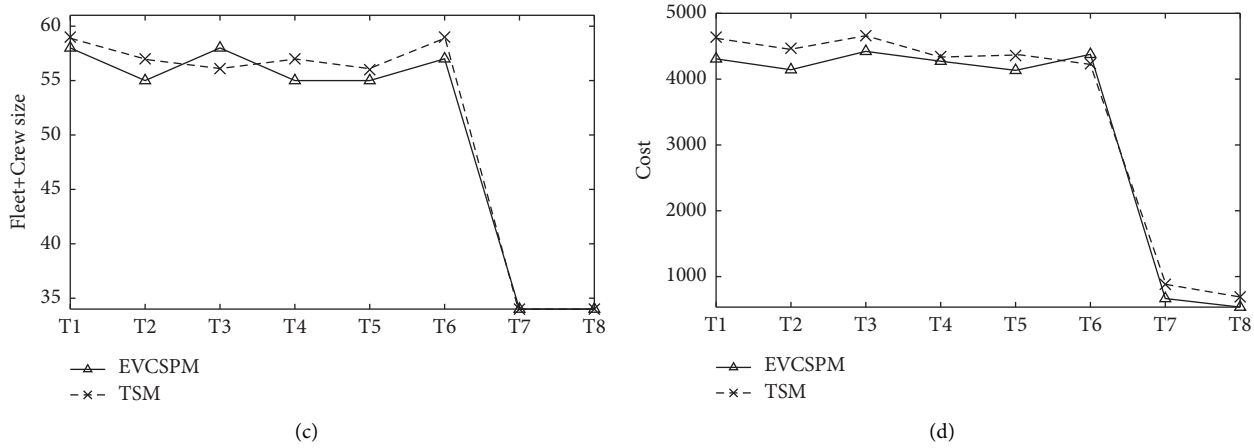

Figure 8: Results produced by EVCSPM and TSM regarding fleet size, crew size, fleet + crew size, and cost.

The impact of coefficients α and β on EVCSPM regarding fleet size and crew size is determined by analyzing T7 with various values of α and β in the [0, 0.06] range. The result is illustrated in Figure 9.

Figure 9 shows that the crew size declines as the value of either α or β increases. This suggests that the fleet size required decreases as α or β becomes larger. When α is held constant, the graph reveals a high absolute slope value for the first surface at β values between 0 and 0.02. This denotes that alterations in β within the given interval significantly influence crew size. Conversely, for α values between 0.02 and 0.06, the first surface displays smoothness, and its slope is zero when beta values exceed 0.03. Consequently, within the range of $\beta \geq 0.02$, any changes made to β basically have no impact on the crew size. Similarly, the second surface displays continuous steepness between 0 and 0.04 for α and β, hence implying that alterations made to both α and β in the given interval have a considerable effect on fleet size. However, when α, $\beta \geq 0.04$, the graph takes a straight line form, indicating that changes made to α and β are incapable of revising the fleet size. To sum up, α perturbs the fleet size, while β affects both the fleet and crew sizes. Nonetheless, these influences vanish when α, $\beta \geq 0.02$, which results in the fleet size and crew size remaining at 17.

The impact of battery capacity E_{full} on the fleet size, crew size, and the number of recharges is analyzed by conducting tests on T1 under fast recharge with varying E_{full} 120~160 kWh, as depicted in Figure 10.

Figure 10 shows that the crew size always remains at 39, regardless of the increase in E_{full}. The changes in E_{full} do not impact the crew size. Moreover, when $E_{\text{full}} \geq 130$ kWh, the fleet size remains constant at 19, while it slightly fluctuates between 19 and 20 in the range of 120~130 kWh. The effect of changes in E_{full} on the fleet size decreases as the capacity takes a smaller value (120~130 kWh), and this effect completely vanishes when $E_{\text{full}} \geq 130$. Additionally, along with the increase in E_{full}, #recharge shows a consistent downward trend. The larger the battery capacity, the fewer recharges are required. #recharge has a relatively slow decline within either 120~135 or 140~160 kWh. However, the number of recharges sharply shrinks from 11 to 5 with an increase in E_{full} from 135 to 140 kWh. Therefore, the changes in E_{full} significantly influence the number of recharges, especially when $135 \leq E_{\text{full}} \leq 140$ kWh. Consequently, it can be inferred that the number of recharges is susceptible to any changes in E_{full}, while the fleet size and crew size remain insensitive. It is worth noting that EVCSP degenerates into VCSP when $E_{\text{full}} \geq 160$ kWh.

Finally, we investigate the impact of recharge power and recharge time on fleet size, crew size, and the number of recharges. To do so, we conduct tests on T1 with various recharge times under $E_{\text{full}} = 140$ kWh, fast-recharge power of 160 kW, and slow-recharge power of 60 kW. We present the findings in Figures 11 and 12.

From Figures 11 and 12, the fleet and crew sizes remain at 19 and 39, respectively, indicating that they are not influenced by recharging power and time. The fleet size displays a decreasing pattern with an increase in recharging time, irrespective of recharging power, whereby fast-recharge power 160 kW or slow-recharge power 60 kW is utilized. The higher the recharging power, the lower the fleet size required. For fast-recharge power 160 kW, the fleet size fluctuates by a maximum of two every 5 min, remaining at 9, 5, and 3 during the time intervals [10, 15], [25, 35], and [50, 60], respectively. Similarly, for slow-recharge power 60 kW, the fleet size varies by a maximum of two every 5 min, remaining at 3 and 1 during the time intervals [50, 60] and [65, 80], respectively. Under the same recharging time, the fleet size remains identical between the two recharging powers, indicating its sensitivity to recharging time and insensitivity to recharging power. However, the cost increases proportionally with an increase in recharging time, irrespective of the recharging power used, whether 60 or 160 kW. The cost increases with an increase in recharging power. For the same recharging time, the cost difference between the two recharge powers is negligible, particularly when $30 \leq T^{rt} \leq 40$ min, indicating that the cost is generally insensitive to recharging time. In conclusion, changes in recharging power and time merely influence the frequency of EV recharges.

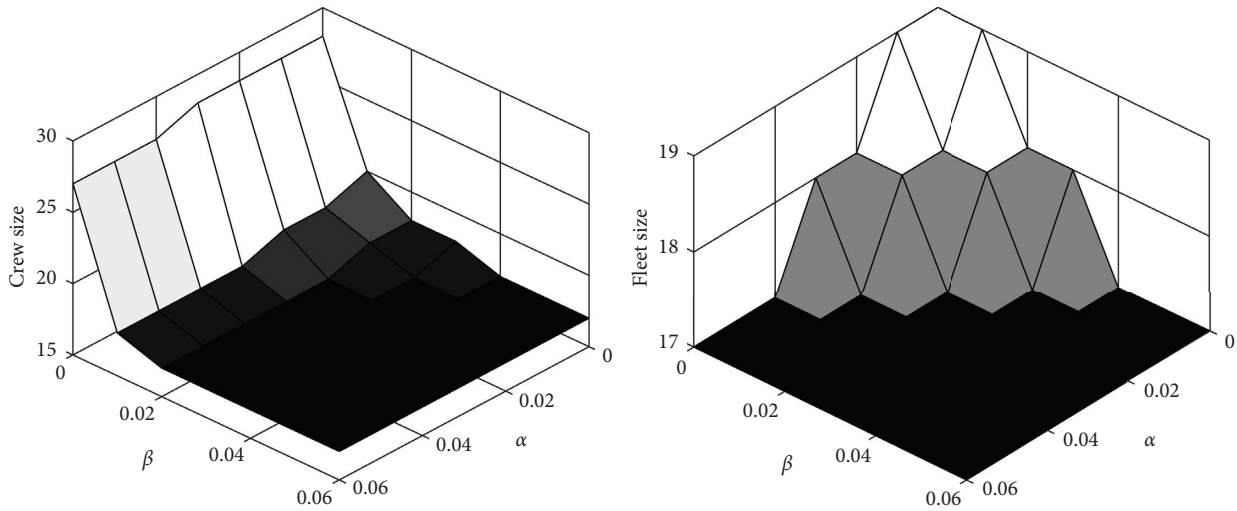

Figure 9: The sensitivity of fleet size and crew size to the changes in α and β.

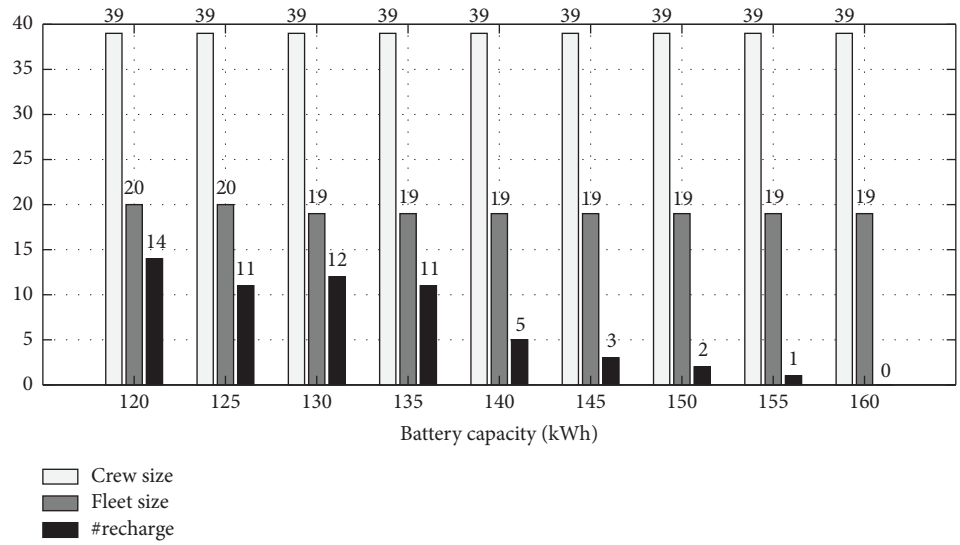

Figure 10: The sensitivity of fleet size, crew size, and number of recharges to the changes in battery capacity. #recharge is the number of recharges.

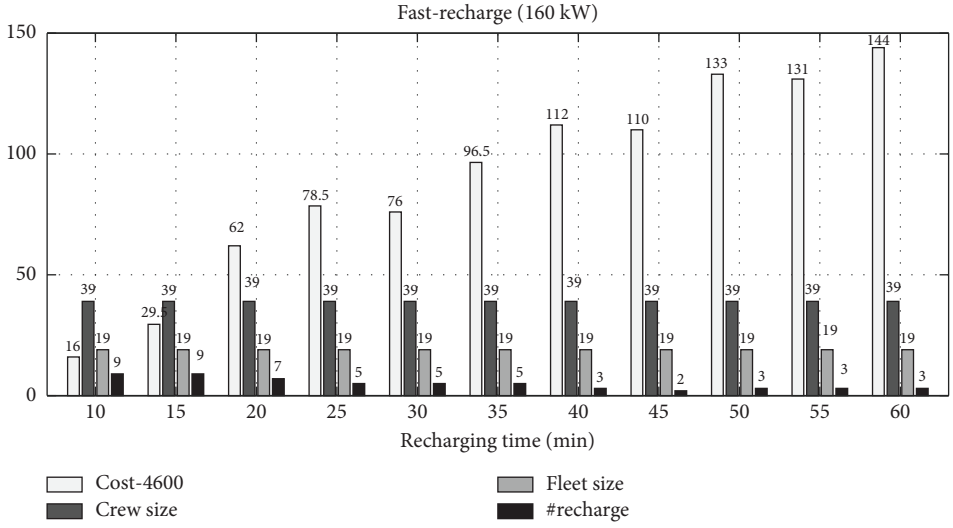

Figure 11: The sensitivity of fleet size, crew size, cost, and the number of recharges to the changes in recharging time under fast-recharge power 160 kW.

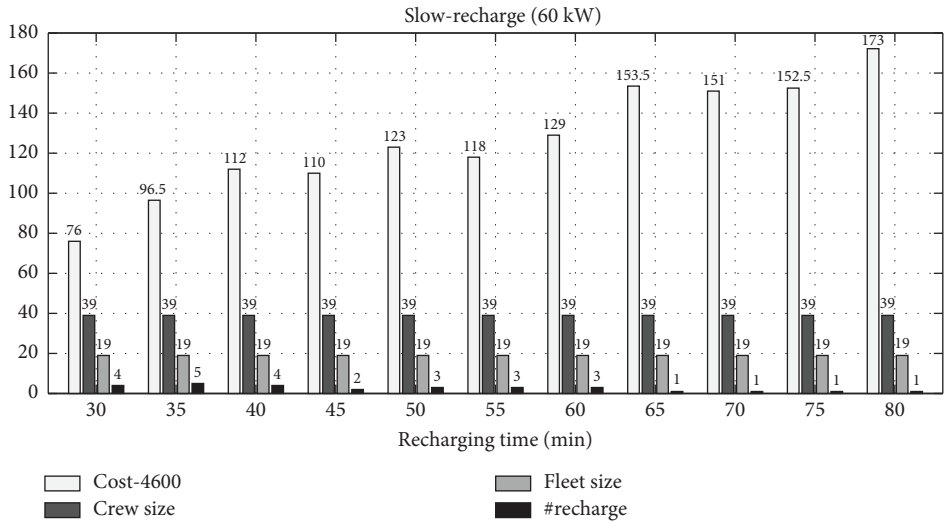

Figure 12: The sensitivity of fleet size, crew size, cost, and the number of recharges to the changes in recharging time under slow-recharge power 60 kW.

7. Conclusions

This paper proposes a complete integrated model, namely EVCSPM, for the electric vehicle (EV) and crew scheduling. EVCSPM is derived based on minimum cost flow. For modeling, we integrate design nodes, directed arcs, cost and constraints, and time and energy compatibility of nodes. A case study has been reported on the real instance of bus route 2 of Xiaogan in Hubei, China (XGR2).

As for comparing EVCSPM with the two-stage sequential model (TSM), it involves the EV scheduling model first and then followed by the crew scheduling model. Based on several problem instances derived from XGR2, EVCSPM outperforms TSM regarding crew size, fleet + crew size, and cost. The average RPDs of crew size, fleet + crew size, and cost are −2.9%, −1.3%, and −8.7%, respectively. Additionally, the average solving time of EVCSPM is approximately one-twentieth of TSM, even the latter overlooks EV energy constraints. The integrated model outperforms the sequential model as it possesses additional flexibility.

None of the integer linear programming (ILP) solvers can be directly used to solve the integrated model since it is the integer nonlinear caused by EV energy constraints and NP-hard for even both sequential subproblems. Therefore, this paper develops a hybrid method that comprises a matching-based heuristic and GUROBI for EVCSPM. Our method approaches the theoretical optimum, but the elapsed time is reduced to 1/60 compared to the ILP solver. Future work involves further exploration of the proposed method and its ability to efficiently overcome larger real-life instances.

Data Availability

All the data included in this study are available upon request by contact with the corresponding author (yindong@hust.edu.cn).

Conflicts of Interest

The authors declare that they have no conflicts of interest.

Acknowledgments

This research was supported by the National Natural Science Foundation of China (Grant nos. 71571076 and 72071087) and the CAAI-Huawei MindSpore Open Fund (CAAIXSJLJJ-2022-034A).

References

[1] Y. Shen, J. Xu, and J. Li, "A probabilistic model for vehicle scheduling based on stochastic trip times," *Transportation Research Part B: Methodological*, vol. 85, pp. 19–31, 2016.

[2] I. Steinzen, V. Gintner, L. Suhl, and N. Kliewer, "A time-space network approach for the integrated vehicle- and crew-scheduling problem with multiple depots," *Transportation Science*, vol. 44, no. 3, pp. 367–382, 2010.

[3] A. Andrade-Michel, Y. A. Ríos-Solís, and V. Boyer, "Vehicle and reliable driver scheduling for public bus transportation systems," *Transportation Research Part B: Methodological*, vol. 145, pp. 290–301, 2021.

[4] D. Huisman, R. Freling, and A. P. M. Wagelmans, "Multiple-depot integrated vehicle and crew scheduling," *Transportation Science*, vol. 39, no. 4, pp. 491–502, 2005.

[5] M. Ball, L. Bodin, and R. Dial, "A matching based heuristic for scheduling mass transit crews and vehicles," *Transportation Science*, vol. 17, no. 1, pp. 4–31, 1983.

[6] N. Kliewer, B. Amberg, and B. Amberg, "Multiple depot vehicle and crew scheduling with time windows for scheduled trips," *Public Transport*, vol. 3, no. 3, pp. 213–244, 2012.

[7] S. Perumal, T. Dollevoet, D. Huisman, R. M. Lusby, J. Larsen, and M. Riis, "Solution approaches for integrated vehicle and crew scheduling with electric buses," *Computers & Operations Research*, vol. 132, no. 2, Article ID 105268, 2021.

[8] R. Deng, Y. Liu, W. Chen, and H. Liang, "A survey on electric buses-energy storage. Power management, and charging scheduling," *IEEE Transactions on Intelligent Transportation Systems*, vol. 22, no. 1, pp. 9–22, 2021.

[9] W. Wu, Y. Lin, R. Liu, and W. Jin, "The multi-depot electric vehicle scheduling problem with power grid characteristics," *Transportation Research Part B: Methodological*, vol. 155, pp. 322–347, 2022.

[10] W. Wu, Y. Lin, Y. Li, W. Jin, and C. Li, "Electric bus scheduling model with stochastic travel time," *China Journal of Highway and Transport*, vol. 36, no. 6, pp. 235–253, 2023.

[11] Y. Shen, Y. Li, C. Chen, and J. Li, "Electric vehicle scheduling based on stochastic trip time and energy consumption," *Computers and Industrial Engineering*, vol. 177, Article ID 109071, 2023.

[12] L. Bodin, B. Golden, A. Assad, and M. Ball, "Routing and scheduling of vehicles and crew-the state of the art," *Computers and Operations Research*, vol. 10, no. 2, pp. 63–211, 1983.

[13] M. Fischetti, S. Martello, P. Toth, and P. Toth, "The fixed job schedule problem with spread-time constraints," *Operations Research*, vol. 35, no. 6, pp. 849–858, 1987.

[14] K. Haase, G. Desaulniers, and J. Desrosiers, "Simultaneous vehicle and crew scheduling in urban mass transit systems," *Transportation Science*, vol. 35, no. 3, pp. 286–303, 2001.

[15] S. Martello and P. Toth, "Generalized assignment problems," in *Proceedings of the International Symposium on Algorithms and Computation*, Nagoya, Japan, December, 1992.

[16] K. Darby-Dowman, J. K. Jachnik, R. L. Lewis, and G. Mitra, "Integrated decision support systems for urban transport scheduling: discussion of implementation and experience," in *Computer-Aided Transit Scheduling*, J. R. Daduna and A. Wren, Eds., vol. 308, pp. 226–239, Springer, Berlin, Germany, 1988.

[17] J. Rousseau and J. Iblais, "HASTUS: an interactive system for buses and crew scheduling," in *Computer Scheduling of Public Transport 2*, J. M. Rousseau, Ed., Springer, Berlin, Germany, 1985.

[18] D. Scott, "A large linear programming approach to the public transport scheduling and cost model," in *Computer Scheduling of Public Transport 2*, J. M. Rousseau, Ed., Springer, Berlin, Germany, 1985.

[19] C. Friberg and K. Haase, "An exact algorithm for the vehicle and crew scheduling problem," *Computer Scheduling of Public Transport 2*, Springer, Berlin, Germany, 1996.

[20] C. Friberg and K. Haase, "An exact branch and cut algorithm for the vehicle and crew scheduling problem," in *Computer-Aided Transit Scheduling Computer Scheduling of Public Transport 2*, N. H. M. Wilson, Ed., vol. 471, pp. 63–80, Springer, Berlin, Germany, 1999.

[21] J. C. Falkner and D. M. Ryan, "EXPRESS: set partitioning for bus crew scheduling in Christchurch," in *Computer-Aided Transit Scheduling: Proceedings of the Fifth International Workshop*, M. D. M. Rousseau, Ed., pp. 359–378, Springer, Berlin, Germany, 1992.

[22] I. Patrikalakis and D. Xerocostas, "A new decomposition scheme of the urban public transport scheduling problem," in *Computer-Aided Transit Scheduling*, M. Desrochers and J. M. Rousseau, Eds., vol. 386, pp. 407–425, Springer, Berlin, Germany, 1992.

[23] E. Tosini and C. Nercellis, "An interactive system for extra-urban vehicle and crew scheduling problems," in *Computer-Aided Transit Scheduling: Proceedings of the Fourth International Workshop*, 1.R. D.A. Wren, Ed., pp. 41–53, Springer, Berlin, Germany, 1988.

[24] K. Haase and C. Friberg, "An exact branch and cut algorithm for the vehicle and crew scheduling problem," in *Computer-Aided Transit Scheduling*, N. H. M. Wilson, Ed., pp. 63–80, Springer, Berlin, Germany, 1999.

[25] D. Klabjan, E. L. Johnson, G. Nemhauser, E. Gelman, and S. Ramaswamy, "Airline crew scheduling with time windows and plane-count constraints," *Transportation Science*, vol. 36, no. 3, pp. 337–348, 2002.

[26] V. Gintner, N. Kliewer, and L. Suhl, "A crew scheduling approach for public transit enhanced with aspects from vehicle scheduling," Technical Report WP0407, University of Paderborn, Decision Support & Operations Research Lab, Paderborn. Germany, 2004.

[27] D. Huisman, "Integrated and dynamic vehicle and crew scheduling (No. 325," Thela Thesis, Tinbergen Instituut Research Series, Amsterdam, Netherlands, 2004.

[28] R. Freling, D. Huisman, and A. Wagelmans, "Models and algorithms for integration of vehicle and crew scheduling," *Journal of Scheduling*, vol. 6, no. 1, pp. 63–85, 2003.

[29] R. Freling, *Models and techniques for integrating vehicle and crew scheduling*, PhD Thesis, Tinbergen Institute, Erasmus University, Rotterdam, Netherlands, 1997.

[30] R. Freling, G. Boender, and J. Paixão, "An integrated approach to vehicle and crew scheduling," Technical Report 9503/A, Econometric institute, Erasmus University Rotterdam, Rotterdam, Germany, 1995.

[31] R. Freling, D. Huisman, and A. Wagelmans, *Models and Algorithms for Integration of Vehicle and Crew Scheduling*, Erasmus Research Institute of Management (ERIM), Rotterdam, Netherlands, 2000.

[32] R. Freling, D. Huisman, and A. Wagelmans, "Applying an integrated approach to vehicle and crew scheduling in practice," in *Computer-Aided Scheduling of Public Transport*, S. Voß and J. R. Daduna, Eds., vol. 505, pp. 73–90, Springer, Berlin, Germany, 2001.

[33] R. Freling, A. Wagelmans, and J. Paixão, "An overview of models and techniques for integrating vehicle and crew scheduling," in *Computer-Aided Transit Scheduling*, N. H. M. Wilson, Ed., vol. 471, pp. 441–460, Springer, Berlin, Germany, 1999.

[34] H. M. Sistig and D. U. Sauer, "Metaheuristic for the integrated electric vehicle and crew scheduling problem," *Applied Energy*, vol. 339, Article ID 120915, 2023.

[35] D. Huisman, R. Freling, and A. Wagelmans, *Multiple-depot Integrated Vehicle and Crew Scheduling*, Erasmus University Rotterdam, Erasmus School of Economics (ESE), Econometric Institute, Rotterdam, Netherlands, 2003.

[36] A. Gaffi and M. Nonato, "An integrated approach to ex-urban crew and vehicle scheduling," in *Computer-Aided Transit Scheduling. Lecture Notes in Economics and Mathematical Systems*, N. H. M. Wilson, Ed., p. 471, Springer, Berlin, Germany, 1999.

[37] M. Mesquita and A. Paias, *Solving Vehicle and Crew Scheduling Problems Simultaneously*, 2004.

[38] M. Mesquita and A. Paias, "Set partitioning/covering-based approaches for the integrated vehicle and crew scheduling problem," *Computers and Operations Research*, vol. 35, no. 5, pp. 1562–1575, 2008.

[39] M. Mesquita, A. Paias, and A. Respício, "Branch-and-price for integrated multi-depot vehicle and crew scheduling problem," in *Proceedings of the Advanced OR and AI Methods in Transportation, 10th EWGT Meeting and 16th Mini-Euro Conference*, Poznan, Poland, September, 2005.

[40] M. Mesquita, A. Paias, and A. Respício, "Branching approaches for integrated vehicle and crew scheduling," *Public Transport*, vol. 1, pp. 21–37, 2009.

[41] D. Huisman and A. Wagelmans, "A solution approach for dynamic vehicle and crew scheduling," *European Journal of Operational Research*, vol. 172, no. 2, pp. 453–471, 2006.

[42] I. Steinzen, M. Becker, and L. Suhl, "Hybrid evolutionary algorithm for the vehicle and crew scheduling problem in public transit," in *Proceedings of the 2007 IEEE Congress on Evolutionary Computation*, Singapore, September, 2007.

[43] R. Borndörfer, A. Löbel, and S. Weider, "A bundle method for integrated multi-depot vehicle and duty scheduling in public," in *Computer-Aided Scheduling of Public Transport, Vol. 600. Lecture Notes in Economics and Mathematical Systems*, M. Hickmann, P. Mirchandani, and S. Voß, Eds., pp. 3–24, Springer, Berlin, Germany, 2008.

[44] S. W. de Groot and D. Huisman, "Vehicle and crew scheduling: solving large real-world instances with an integrated approach," in *Computer-aided Systems in Public Transport. Lecture Notes in Economics and Mathematical Systems*, M. Hickman, P. Mirchandani, and S. Voß, Eds., p. 600, Springer, Berlin, Germany, 2008.

[45] L. Kang, S. Chen, and Q. Meng, "Bus and driver scheduling with mealtime windows for a single public bus route," *Transportation Research Part C: Emerging Technologies*, vol. 101, pp. 145–160, 2019.

[46] A. Kéri and K. Haase, "Simultaneous vehicle and crew scheduling with trip shifting," in *Operations Research Proceedings 2007*, J. Kalcsics and S. Nickel, Eds., Springer, Berlin, Germany, 2008.

[47] M. Mesquita, M. Moz, A. Paias, J. Paixão, M. Pato, and A. Respício, "A new model for the integrated vehicle-crew-rostering problem and a computational study on rosters," *Journal of Scheduling*, vol. 14, no. 4, pp. 319–334, 2011a.

[48] M. Mesquita, M. Moz, A. Paias, and M. Pato, "A decomposition approach for the integrated vehicle-crew-roster problem with days-off pattern," *European Journal of Operational Research*, vol. 229, no. 2, pp. 318–331, 2013.

[49] B. Amberg, B. Amberg, and N. Kliewer, "Robust efficiency in urban public transportation: minimizing delay propagation in cost-efficient bus and driver schedules," *Transportation Science*, vol. 53, no. 1, pp. 89–112, 2019.

[50] B. Amberg and B. Amberg, "Robust and cost-efficient integrated multiple depot vehicle and crew scheduling with controlled trip shifting," *Transportation Science*, vol. 57, no. 1, pp. 82–105, 2023.

[51] M. Horváth and T. Kis, "Computing strong lower and upper bounds for the integrated multiple-depot vehicle and crew scheduling problem with branch-and-price," *Central European Journal of Operations Research*, vol. 27, no. 1, pp. 39–67, 2019.

[52] E. M. L. Simões, L. D. S. Batista, and M. J. F. Souza, "A matheuristic algorithm for the multiple-depot vehicle and crew scheduling problem," *IEEE Access*, vol. 9, pp. 155897–155923, 2021.

[53] B. Laurent and J. K. Hao, "Simultaneous vehicle and driver scheduling: a case study in a limousine rental company," *Computers and Industrial Engineering*, vol. 53, no. 3, pp. 542–558, 2007.

[54] B. Laurent and J. K. Hao, *Simultaneous Vehicle and Crew Scheduling for Extra Urban Transports*, Springer, Berlin, Germany, 2008.

[55] V. Boyer, O. J. Ibarra-Rojas, and Y. Á. Ríos-Solís, "Vehicle and crew scheduling for flexible bus transportation systems," *Transportation Research Part B: Methodological*, vol. 112, pp. 216–229, 2018.

[56] B. Prata, T. G. Dias, and J. Sousa, *A Maximum Covering Modeling for Integrated Vehicle Scheduling without Change-overs. Business*, 2013.

[57] B. de Athayde Prata, "A hybrid Genetic Algorithm for the vehicle and crew scheduling in mass transit systems," *IEEE Latin America Transactions*, vol. 13, no. 9, pp. 3020–3025, 2015.

[58] B. Prata, "A multiobjective metaheuristic approach for the integrated vehicle and crew scheduling," *Journal of Transport Literature*, vol. 10, no. 2, pp. 10–14, 2016.

[59] H. Pan, Z. Liu, L. Yang, Z. Liang, Q. Wu, and S. Li, "A column generation-based approach for integrated vehicle and crew scheduling on a single metro line with the fully automatic operation system by partial supervision," *Transportation Research Part E: Logistics and Transportation Review*, vol. 152, Article ID 102406, 2021.

[60] J. Q. Li, "Transit bus scheduling with limited energy," *Transportation Science*, vol. 48, no. 4, pp. 521–539, 2014.

[61] M. Wen, E. Linde, S. Ropke, P. Mirchandani, and A. Larsen, "An adaptive large neighborhood search heuristic for the Electric Vehicle Scheduling Problem," *Computers and Operations Research*, vol. 76, pp. 73–83, 2016.

[62] A. Alfieri and G. Nicosia, "Minimum cost multi-product flow lines," *Annals of Operations Research*, vol. 150, no. 1, pp. 31–46, 2007.

[63] H. S. Shih and E. S. Lee, "Fuzzy multi-level minimum cost flow problems," *Fuzzy Sets and Systems*, vol. 107, no. 2, pp. 159–176, 1999.

[64] M. W. Fontana, "Optimal routes for electric vehicles facing uncertainty, congestion, and energy constraints," Doctoral Dissertation, Massachusetts Institute of Technology, Massachusetts, MA, USA, 2014.

[65] Y. Shen, K. Peng, K. Chen, and J. Li, "Evolutionary crew scheduling with adaptive chromosomes," *Transportation Research Part B: Methodological*, vol. 56, no. 56, pp. 174–185, 2013.

[66] D. Huisman, R. Freling, and A. Wagelmans, "A robust solution approach to the dynamic vehicle scheduling problem," *Transportation Science*, vol. 38, no. 4, pp. 447–458, 2004.

[67] Y. Shen, *Two Neighbourhood Search Approaches: 2-opt Heuristics and Tabu Search for Bus and Train Driver Scheduling*, vol. 10, Science Press, Beijing, China, 2003.

[68] A. A. Bertossi, P. Carraresi, and G. Gallo, "On some matching problems arising in vehicle scheduling models," *Networks*, vol. 17, no. 3, pp. 271–281, 1987.

[69] R. P. Dilworth, "A decomposition theorem for partially ordered sets," *Annals of Mathematics*, vol. 51, no. 1, pp. 161–166, 1950.

[70] X. Tang, X. Lin, and F. He, "Robust scheduling strategies of electric buses under stochastic traffic conditions," *Transportation Research Part C: Emerging Technologies*, vol. 105, pp. 163–182, 2019.

[71] O. J. Ibarra-Rojas, F. Delgado, R. Giesen, and J. C. Munoz, "Planning, operation, and control of bus transport systems: a literature review," *Transportation Research Part B: Methodological*, vol. 77, pp. 38–75, 2015.